Response to Anonymous Referees

"Overview: Precipitation Characteristics and Sensitivities to Environmental Conditions during GoAmazon2014/5 and ACRIDICON-CHUVA" by Luiz A. T. Machado et al.

Dear Editor,

The authors would like to thank the two reviewers for their helpful comments and suggestions. We have responded to each reviewer comment and incorporated the reviewer suggestions into the manuscript.
The individual reviewer comments and responses are included below, with author comments in **bold** and reviewer comments in *italics*.

Response to Referee #1 – Dr. Y. Zhuang.

We would like to thank Dr. Y. Zhuang for the valuable comments (*italic*). We will improve the manuscript based on your suggestions. Please find a point-by-point response (**bold**) and proposed changes to the manuscript below.

This study utilized field campaign data collected during GoAmazon 2014/5 and CHUVA-ACRIDICON, as well as satellite and S-band radar data, to give an overview of precipitation characteristic and corresponding thermodynamic conditions, and analyze the relationship between precipitation and several environmental conditions, including aerosol loading, land surface, etc. Contrast between the wet and dry season for these characteristics and relationship were emphatically discussed. Although there are numerous previous studies about the convection and precipitation in the Amazon, this is the first paper which summarizes such complex features about the precipitation and its seasonality in the Central Amazon using multiple comprehensive datasets. Overall, I found this work to be well-written and scientifically sound, and results in this work will aid to further understanding of cloud and precipitation systems in Amazon and potentially provide implications for modeling groups to improve GCM parameterization. I recommend this manuscript to be published after some minor revisions.

Thank you for your comments. The manuscript was improved based on your recommendations.

Specific Comments:

1. *Page 3, Line 10: Could the authors provide reference for this statement? Additionally, I think it would be also helpful to add monthly rainfall in Figure 2 since SIPAM product is available in 2014 and 2015 whole year. In ECMWF reanalysis data and S band radar rain rate derived by (Zhuang et al. 2017, JGRA), Sep is even drier than July and August.*

The reference is Machado et. al. (2004) DOI 10.1007/s00704-004-0044-9. In this case, we are referring to Manaus (data were obtained from rain gauges). You are correct that September is drier than July and that August is the driest month. September was added to the text. We added an additional Figure (Fig. 2F) to show the 2014 monthly mean rainfall and rainfall rates. We believe that it is more appropriate to use the rain gauge data in this instance. The SIPAM S-band radar data are discussed in item 3, and 2014 was chosen to reflect the same period shown in the other panels of Figure 2.

2. *Page 3, Line 15: It would be helpful to describe how CAPE was calculated either here or in the method section. Specifically, what is the initial condition of the parcel (surface based, mixed layer average, . . .)? The choice of initial parcel could affect the CAPE value very significantly, possibly the seasonality as well.*

We added the thermodynamic calculation procedures to the methodology based on your suggestion. This procedure relied on surface calculations. The Williams et al.

paper also relied on surface data to compute CAPE (this information was also included in the text).

3. *Page 7, Line 12: Is there a reason for only using 2014 wet-season disdrometer data to determine the Z-R relationship? Can the authors further speculate how much this approximation that the wet and dry seasons have same DSD could affect results? Such as Figure 1 and Figure 4, does the approximation make the difference between wet and dry season smaller or larger?*

There was a mistake in the legends for Figures 4 and 7; the rainfall data were collected using a disdrometer, as explained in the text. The effect of the radar S-band rainfall estimation is only considered in Figures 8 and 12. As these figures are presented by vegetation and topography class for each season, the Z-R relationship has little effect on the conclusions. Therefore, the variation between the classes rather than the absolute values should be considered. We used the Joss disdrometer and the period with the best data (i.e., the wet season with the J-W) to create the Z-R relationship. A sentence was added to the text discussing the possible implications of this method on the total rainfall measurements.
The Z-R relationship is more sensitive to the way one filters out disdrometer data than to the intrinsic difference between the wet and dry Z-R relationship. Thus, this relationship was considered by ARM-DOE as more appropriate (Courtney Schumacher, data mentor). The Joss disdrometer was only used during the wet season by the researchers because they were considering a more continuous and larger sample than previously collected. The researchers filtered out all points with less than 100 droplets per minute. This method resulted in a more conservative relationship that is closer to Marshall Palmer. However, if a filter of 10 drops per minute is considered, the Z-R relationship differs more substantially than can be explained by the wet-dry seasonal differences. Figure 1 shows some of the Z-R relationships used to test the ARM Z-R relationship. IOP2-JW is the Joss adjusted relationship during the dry season (filter 10 drops/minute); IOP1-JW is the Joss-adjusted relationship during the wet season (filter 10 drops/minute); and Aaron is the relationship used in the manuscript and in the ARM database (for wet Joss but filtered using 100 drops per minute). The Marshall Palmer (MP) and NEXRAD were also considered. Note that differences between how the disdrometer data are filtered are larger than the differences between dry and wet seasons when using the same filter. We added a discussion within the text explaining why the S-band data were not considered as an absolute value of rainfall.

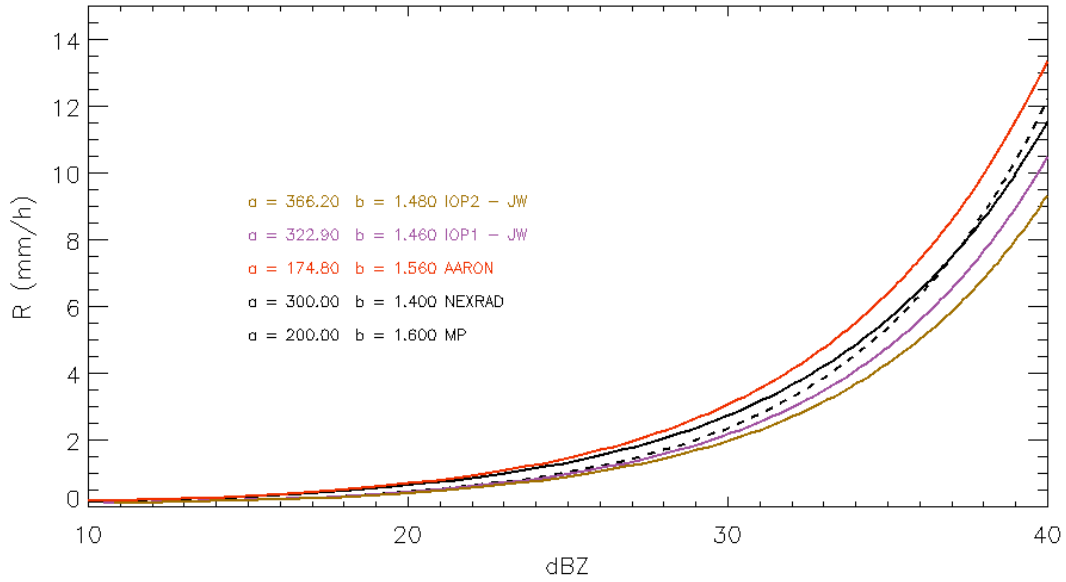

4. *Page 9, Line 21-22: I feel that usage of "rain rate" and "rainfall" could be a little confusing here. By "This is the reason why the wet season has a maximum rain rate", I think the authors actually mean the average daily rain rate but not the rain rate used in Line 15-16 for rain event. I feel it's better to explicitly specify the average period and use something like "rain rate for precipitation event", or just use symbol RR and R to discriminate them. Also check Line 34 in abstract and description in Figure 1.*

We were trying to explain the exception (the largest RR occurred during the wet season – only one case) and in doing so created confusion, as you noted. We rewrote this part to clarify our meaning and have taken your other suggestions into consideration.

5. *Page 9, Line 30-33: Similar conclusions about atmospheric instability and cloud fraction variations between wet and dry season were also discussed in some previous studies such as Zhuang et al. 2017.*

The reference was added to the text.

6. *Page 9, Line 31: Definition of bulk shear is not given. Is it surface to 6km bulk shear?*

The definitions of all the thermodynamic-dynamic parameters were added to the methodology. The bulk shear is the difference between the surface-500 m and surface-6000 m average wind speed.

7. *Page 12, Line 24-26: Is the comparison "clearer distinction" made between the dry and wet season or between 8km and above 8km in the dry season? Also, in conclusion section at Page 17, Line 28-29, ". . . more homogenous clouds above 8-km . . .", does this contradict with ". . . higher correlation at approximately*

8km" here? It seems to me the frequency of RhoHV<0.97 is higher above 8km, and that of RhoHV>0.97 is lower above 8km. Doesn't this mean the average RhoHV is smaller and the cloud becomes less homogenous above 8km?

The clearest distinction appears below and above 8 km. This was clarified in the text. You are correct that the sentence was not well written, which resulted in an incorrect interpretation. The text was changed to "During the dry season, there appears to be a clearer distinction between the mixed phase and the glaciation phase above 8 km. The wet season correlation coefficient is more homogenous with height inside the cloud."

8. *Comparison between Figure 6c and 6f shows dry season has larger frequency in high RhoHV range (larger purple area) above melting layer and below 8 km, which means RhoHV is smaller and the cloud becomes less homogenous above 8km.*

We agree and have addressed this item as discussed in item 7. The paragraph has been rewritten. We hope the new text is clearer and more accurate.

9. *Page 14, Line 19-22: Discussions here are not very clear. What does "the variation . . . is 25%" mean? What "difference" is "very consistent"?*

Yes; this sentence requires clarification. We intended to refer to the difference between the RR median values of each surface type. In addition, the data are not consistent but are significant. This was changed in the text.

10. *Page 16, Line 2: "difference . . . increase with the altitude . . .". I don't find this statement to be true for Figure 11b.*

You are correct that the results are only clear for leg 1. This correction was made in the text. The time of leg 1 compared with leg 2 (later, when the convective boundary layer was fully developed) resulted in this difference, which has been clarified in the text.

11. *Page 16, Line 20: Please provide statistical test for the linear relationship in Figure 10, especially 10c. In addition, solid rectangles and circles look very similar in Figure 10bc. Maybe use another marker such as "x" in Figure 10a.*

The statistical information (correlation) was revised in the text. As the correlation is only around 0.6, we changed the sentence from nearly linearly related to more linearly related than the vertical velocity.

12. *Page 16, Line 30-31: Firstly, although dry season seems to have a stronger linear dependency between rainfall and elevation than the wet season, they still look very similar. Is this difference significance tested between all adjacent elevation groups? Similarly, it would be helpful to indicate if the difference passes the significance test between different surface types for a single season in Figure 8. Secondly, the conclusions here about the dependency of dry season*

rain rate on topography seem to valid at first. However, is this result independent from those in section 3.2.2 about surface type? If so, the authors need to indicate there is no specific relationship between surface type and topography. I also suggest adding a figure to show surface type and contoured elevation of the studied area.

We agree that it is more appropriate to test significant differences among the classes than between the seasons. We have tested the differences among the classes, and all differences during the dry season were significant. However, we continued our analysis of this difference using the T-student parametric test. We were curious why all classes passed the test and identified important discussion points related to parametric significance tests in very large sample sizes. These comparisons were done for several days at the pixel level, so the sample set is very large. All tests generally pass under this condition, and there is no statistical way to use the test with such a large sample set. By using box plots, all basic statistics are shown. Therefore, we decided to eliminate the T-student test for vegetation and topography. This test was only valid when we tested T3 site-specific data, which resulted in a much smaller sample set. We eliminated the arrows in Figure 9 (new, formerly 8) and 13 (new, formerly 12).

13. Page 18, Line 21: Could the authors provide reference to the related studies?

A reference was added to the text.

14. Quality of some figures need to be improved. Specifically, e.g., sub-figures were not properly labelled, such as Figure 3-6 & 9; black lines around the figure should be removed, such as Figure 3&6; Figure 2, Maybe more details about the box plot can be given either in text, figure caption, or both. e.g. how is "outlier" defined and how to determine the length of whiskers?; text "wet" and "dry" are not all visible inside the Figure 6; Figure 10a is in different size with 10bc; some texts were not shown as subscripts, such as Nccn and Dm; etc.

The sub-figures are now labeled The frame was a placeholder in the manuscript. The figures will be provided individually, and the Journal will organize according to their standards. Details about the box plots were added to the text. The "Wet" and "Dry" labels in Figure 6 are now visible. The size of Figure 10 was changed.

15. I'm not sure how to interpret the unit (%) of occurrence frequency in Figure 5&6. If the CFAD was constructed the same way as (Yuter and Houze, 1995, Part II, MWR), shouldn't the unit be, for example, "% km-1 dBZ-1" for Figure 6ac.

The CFAD was constructed as follows: each CFAD consists of a PDF of reflectivity at each height multiplied by 100 so that the values are presented as percentages. The CFAD calculation used 2 dBZ-bin and 0.4 km-bin intervals. After the first paper (Yuter and Houze, 1995), the others papers that use CFAD rely on this explanation. We added this sentence to the legend and the intervals.

Typos and Grammar Issues includes, but is not limited to:

Page 1, Line 28: "This is study" –> "This study"

Changed as recommended.
Line 30: "instruments systems" –> "instrument systems"
Changed as recommended.
Line 32: "have carefully been" –> "have been carefully"
Changed as recommended.
Line 35: "While" cannot be used to start the sentence here
Changed as recommended.
Page 2, Line 1: "as well" –> "as well as", "among" –> "between"
Changed as recommended.
Line 2: "analyse" –> "analyzed"
Changed as recommended.
Line 3: "is" –> "was"
Changed as recommended.
Line 7: "observe" –> "observed", "dependence on" –> "dependence of"
Changed as recommended.
Line 10: "cloud droplets number" –> "cloud droplet number"
Changed as recommended.
Line 10-11: "revealed", "exhibit" check tense consistency
Changed as recommended.
Line 20: "sea -level" –> "sea level"
Changed as recommended.
Page 3, Line 10: "Amazonas, For" –> "Amazonas. For"
Changed as recommended.
Page 4, Line 20: "During" –> "during"
Changed as recommended.
Page 6, Line 20: "present" –> "presents"
Giangrande et al., so present is correct.
Line 25: "Section two" –> "Section 2"
Changed as recommended.
Page 9, Line 16: "differences, the" –> "differences. The"
Changed as recommended.
Page 10, Line 6: "Cloud Clusters and Rain Cells-Size Distribution" –> "Size Distribution of Cloud Clusters and Rain Cells"
Changed as recommended.
Line 27: "diameter" –> "Diameter"
Changed as recommended.
Page 11, Line 4: "present" –> "presented"
Changed as recommended.
Line 17: "function" –> " functions"
Changed as recommended.
Page 14, Line 21: "few differences" –> "smaller differences"?
Changed to smaller differences.
Page 15, Line 34: "difference" –> "different"
Changed as recommended.
Page 17, Line 25: remove "Conversely, "
Changed as recommended.
Page 30, Figure 1: Label for x-axis should be "mm ï´Cd¯h-1" not "mm.h-1". Also check

other figures. Use “Sep” instead of “Sept”.
Changed as recommended
Page 32, Figure 3: “distributions between wet and dry seasons and the difference between dry . . .” –> “distributions during the wet and dry seasons and the difference between the dry . . .”
Changed as recommended.
Page 33, Figure 4: “t-statistic” –> “t-test”
Changed as recommended.
Page 36, Figure 7: “radar S-band” –> “S-band radar”
This part was eliminated as explained in item 3.
Page 37, Figure 8: “t-student” –> “Student’s t-test”
Changed as recommended.

Response to Anonymous Referee #2.

We would like to thank you for your valuable comments (*italic*). We will improve the manuscript based on your suggestions. Please find a point-by-point response (**bold**) and proposed changes to the manuscript below.

This paper uses satellite and in situ data from two recent field campaigns to provide an overview of precipitation characteristics in the central Amazon, and their sensitivity to environmental conditions including time of year (wet vs dry season), aerosol concentrations, land-surface type and topography. The paper describes the complex interactions between different processes in the region, particularly through their impact on cloud microphysics, in a way which is only made possible by these new measurements. While the broad scope of the paper means that each aspect cannot be explored in a lot of detail, it still provides interesting results while also show casing the potential of these new datasets for further work. The paper is well organized and mostly well written (some grammar issues aside), and I recommend it for publication after addressing the following fairly minor comments.

Thank you for your comments and suggestions. All points were addressed as described below.

General comments
Language:
While the paper is perfectly readable and understandable, there are minor grammar errors throughout – these do add up to quite a large number, which is why I haven't listed them below. I would encourage a thorough proofread by a native speaker.

The manuscript has been reviewed by American Journal Experts, an English-language editing service. We hope this has improved the grammar throughout the paper.

Introduction:
This is quite long (about a quarter of the whole paper), although it is very comprehensive. I don't think it's a major issue, but worth pointing out.

We agree that the Introduction is long for a conventional manuscript; however, because we are treating the introduction as an overview, we wished to describe what is known about cloud processes in the Amazon as determined from the field campaign so far. This is why we split the Introduction in two sub-sections. We hope this structure is acceptable as is.

Methods:
Given one of the aims of the paper is to show case a new dataset, it is really lacking in contextual information, including where exactly the whole experiment is taking place. If the instruments are all exactly collocated simply the latitude/longitude might be ok, but I would strongly encourage you to include a map somewhere, showing the location of

the instruments (particularly if placed at different locations), as well as the flight paths. This would also allow you to add some much need context.

There are two papers that discuss the details of the GoAmazon campaign: Introduction: Observations and Modeling of the Green Ocean Amazon (GoAmazon2014/5) by Martin et al. (2016) (doi:10.5194/acp-16-4785-2016) and The Green Ocean Amazon Experiment (GoAmazon2014/5) Observes Pollution Affecting Gases, Aerosols, Clouds, and Rainfall over the Rain Forest by Martin et al. (2015) (doi:10.1175/BAMS-D-15-00221.1). We understand that the manuscript should be read independently from others papers; however, both papers were included in a special issue, and the introductory paper provides all of the descriptions about the project. Martin´s Figures 1 and 2 provide the information you request. In the beginning of the methodology, we reference these specific figures in order to provide the reader with a general description of the sites and flights.

I would suggest including land surface type, topography and maybe potentially mean winds/some other climatological data.

We added a figure (new Figure 8) indicating the radar-covered area, the vegetation and topography relative to T3 and the SIPAM radar.

State more precisely in the abstract where the experiment is taking place (i.e. not just 'Central Amazon Basin', but ' in the vicinity of Manaus' or something like that).

Changed as recommended.

Land surface results (3.2.2/3.2.3): while these results are interesting as a very general overview, I think it is difficult to draw particularly strong conclusions from them. Firstly, I'm not sure in Figure 8 there really is 95% confidence that the results are different; the test assumes all data points are independent, which will clearly not be the case. The most obvious example is the 'urban area', which accounts for only 0.5% of points – presumably these points are all clustered together, and likely to be highly autocorrelated. Even if the differences were significant, potential cofounding factors are not considered at all by the authors. For example, topography and land surface type could be correlated in some way, in which case it wouldn't be clear which factor was really driving the differences.

We have revised the figure to illustrate the vegetation and topography distributions. The data are not correlated, and forest covers much of the area. We computed the T-student test for the vegetation and topography to identify the difference between seasons, but the best method would be to test the difference among the classes, as stated by reviewer 1.

We agree with reviewer 1 that it is more appropriate to test significant differences among the classes than between the seasons. We have tested the differences among classes, and all differences in the dry season were significant. Furthermore, we used the T-student parametric test. We were curious why all classes passed the test and identified important discussion points related to parametric significance tests when using very large sample sizes. These comparisons were done for several days at the

pixel level, so the sample set is very large. All tests generally pass under this condition, and there is no statistical way to use the test with such a large sample set. By using box plots, all basic statistics are shown. Therefore, we decided to eliminate the T-student test for vegetation and topography. This test was only valid when we tested T3 site specific data, which resulted in a much smaller sample set. We eliminated the arrows in Figure 9 (new, formerly 8) and 13 (new, formerly 12).

Finally, the explanation of physical mechanisms is sometimes inconsistent. In particular, p14, L24-26 states that the urban heat island over Manaus will drive convergence and enhanced rainfall, while reduced latent heating will decrease rainfall over non-forest. These statements are interchangeable – cities have reduced latent heating, and the non-forest will be warmer, so why do they have opposite feedbacks?

The answer to your question involves the scale. There is a forest around Manaus, so the city will be warmer and receive moisture convergences from the forest. However, there is little moisture convergence from large deforested regions during the dry season because these regions have no moisture source to support this process (if the deforested area is large). We attempted to explain this scale problem and discuss the cautions that need to be taken when considering these physical explanations because scale impacts our discussion. The text was revised in the vegetation section to address this concern.

Minor comments
P9, L18-19: "Figure 1 clearly reveals. . ." Looking at figure 1 it looks to me like the only bin where the wet season is higher is the lowest one (and marginally, the second), which represent RR < 5.
This is a logarithmic scale; however, we have deleted the word "clearly."

P11, L20: "This result suggests. . ..the wet season" I don't quite understand this sentence.
This sentence has been removed.

P13, L14-15: "During the dry season. . .mostly by drier days". Might be useful to add a short comment as to why? Presumably this is because biomass burning is more likely to occur on dry days? More broadly, some comments on what the different sources are for the aerosol you measure would be useful.

We introduced a sentence with this discussion and added a reference that describes the aerosol types.

P13, L19: What was the significance level? I think it's fine to discuss the results even if the significance is below 95% if they are still physically consistent, but there is still a difference between, for example, 80% significance and no correlation whatsoever.

We computed the significance (85%) and added it to the text.

P15, L21-28: if clouds were at different heights over forest and non-forest, could your fixed-height measurements simply be a reflection of what part of the cloud you were measuring, instead of the clouds having different microphysical properties over different surfaces?

You are suggesting that clouds over forest have a different cloud base than those over non-forest. This is true; however, we are not certain if this occurs within such a short path as those in this study (around 50 km). That said, the first leg occurred in the morning when the cloud base difference is very small. There was a cloud base flight (just below) prior to the level 1500. We have added a discussion about this possible effect on the measurements in the text.

Figure 1: it would be nice to have error bars (these could replace the squares and circles). I would only refer to the 'T3 site' in the caption if its location is defined in the text (not just with a reference).

Figure 1 is a frequency distribution; therefore, it is not possible to add error bars. However, we added a new Figure 2f, which shows the rain rate box plots.

Figure 6: It would be helpful to state in the caption roughly what ZDR, KDP and horizontal-vertical correlation refer to physically (e.g. ice orientation for ZDR).

Changed as recommended.

Overview: Precipitation Characteristics and Sensitivities to ~~the~~ Environmental Conditions during GoAmazon2014/5 and ACRIDICON-CHUVA

Luiz A. T. Machado[1], Alan J. P. Calheiros[1], Thiago Biscaro[1], Scott Giangrande[2], Maria A. F. Silva Dias[3], Micael A. Cecchini[3], Rachel Albrecht[3], Meinrat O. Andreae[4,14], Wagner F. Araujo[1], Paulo Artaxo[5], Stephan Bormann[4], Ramon Braga[1], Casey Burleyson[6], Cristiano W. Eichholz[1], Jiwen Fan[6], Zhe~~ng~~ Feng[6], Gilberto F. Fisch[8], Michael P. Jensen[2], Scot T. Martin[7], Ulrich Pöschl[4], Christopher Pöhlker[4], Mira L. Pöhlker[4] Jean-François Ribaud[1], Daniel Rosenfeld[9], Jaci M. B. Saraiva[10], Courtney Schumacher[11], Ryan Thalman[12] David Walter[4] and Manfred Wendisch[13]

[1]National Institute for Space Research (INPE), Sao José dos Campos, Brazil
[2]Brookhaven National Laboratory, Upton, New York, USA
[3]Institute of Astronomy, Geophysics, and Atmospheric Sciences, University of São Paulo, Brazil
[4]Max Planck Institute for Chemistry, Mainz, Germany
[5]Institute of Physics, University of São Paulo, São Paulo, Brazil
[6]Pacific Northwest National Laboratory, Richland, WA
[7]Harvard University, Cambridge, Massachusetts, USA
[8]Department of Aerospace Science and technology
[9]Hebrew University of Jerusalem, Israel
[10]Amazon Protection System (SIPAM), Manaus, Brazil
[11]Texas A&M University, College Station, Texas, USA
[12]Snow College, USA
[13]Leipzig Institute for Meteorology, Leipzig University, Leipzig, Germany
[14]Scripps Institution of Oceanography, University of California San Diego, CA 92037, USA

Correspondence to: Luiz A. T. Machado (luiz.machado@inpe.br)

Formatado: Português (Brasil)

Abstract. This study provides an overview of precipitation processes and their sensitivities to environmental conditions~~,~~ in the Central Amazon Basin~~, in the vicinity of~~ near Manaus~~,~~ during the GoAmazon2014/5 and ACRIDICON-CHUVA experiments. This study takes~~aking~~ advantage of the numerous ~~measuring~~ measurement platforms and instrument systems operating during both campaigns to sample~~ing~~ cloud structure and environmental conditions during 2014 and 2015~~;, the~~ the rainfall variability among seasons, aerosol loading, land surface type, and topography have been carefully characterized using these data. Differences between the wet and dry seasons were examined from a variety of ~~different~~ perspectives. The rainfall rates ~~distribution~~distribution, ~~the~~ total amount of rainfall, and ~~the~~ raindrop size distribution (the ~~mean~~ mass-weighted mean diameter) were quantified over both~~for the two~~ seasons. The dry season generally exhibited~~has typically~~ higher rainfall rates than the wet season and included~~reflects~~ more intense rainfall periods. However, the cumulative rainfall during the wet season

rainfall amount was four times larger greater than that during the total dry season rainfall, reflecting in largeas shown in the total rainfall accumulation data. The typical size and life cycle of the Amazon cloud clusters (observed by satellite) and rain cells (observed by radar) were examined, as well as theirwere differences in these systems between the seasons. Moreover, we analysed the monthly mean thermodynamical and dynamical variables were analysed using, measured by radiosondes to elucidate the differences in rainfall characteristics during the wet and dry seasons. The sensitivity of rainfall to the atmospheric aerosol loading was discussed with regard to the mean mass-weighted mean diameter and rain rate. This topic was only evaluated only during the wet season only due to the insignificant statistics of rainfall events for different ranges of aerosol loading rangess and the low frequency of precipitation events during the dry season. The impacts of aerosols impacts on the cloud droplet diameter varied based on droplet sizeis different for small and large drops. For the wet season, we observed no dependence betweenof land surface type andon the rain rate. However, during the dry season, urban areas exhibited the largest rainfall rate tail distribution, and deforested regions exhibitedhave the lowest mean rainfall rate. Airplane measurements were performed taken to characterize and contrast cloud microphysical properties and processes over forested and deforested regions. VThe vertical motion turned out to be uncorrelatedwas not correlated with cloud droplet sizes, but the cloud droplet number concentration correlatedrevealed a linearly with relationship to the vertical motion. Clouds over forested areas contained exhibited larger droplets than clouds over pastures at all altitudescloud levels. Finally, the connections between topography and rain rate were evaluated, withshowing a higher rainfall rates identified at over higher elevations duringfor the dry season.

1. Introduction

1.1 - The Amazon Forest Climate

The Amazon Forest is a huge area spansning more than 3,000 km in the east-west direction and approximately 2,000 km from north to south. It crosses theThe equator crosses the region, whichbut is primarily located in the Southern Hemisphere and encompasses both equatorial and tropical climates. Additionally, tThe northern expansepart of the Amazon Bbasin is influenced by the tropical Atlantic Ocean, while the western edge is dominated by the Andes Mountains, which rise more than 4,000 m above sea level in the tropical and equatorial regions.

Cavalcanti et al. (2009) have providedpresented a detailed picture of weather and climate in Brazil, particularly in the Amazon. The dominant large-scale features in the Amazon areis the lack of major temperature gradients and the absence of baroclinic weather systems. However, this doesthese features do not mean that there is a lack of convective organization. The main synoptic systems that approach the region and alter the weather conditions are: a) the Intertropical Convergence Zone, mostly affecting the northern half of the Amazon; b) the easterly waves coming from the tropical Atlantic (Diedhiou et al., 2010); c) the upper tropospheric cyclonic vortices originating on the eastern coast of northeast Brazil and the associated upper air Bolivian High (Silva Dias et al., 1983 and Kousky and Gan, 1981); d) the South Atlantic Convergence Zone, which affectsing the southern half of the Amazon and, which has a major effect on the Amazonian convective activity as a whole (Rickenbach et al., 2002); and e) the northward propagation of convective clouds (Siqueira and Machado, 2004) and the remnants of mid-

latitude cold frontal systems that may propagate northward, sometimes beyond the equator, resulting in so called “friagem” events (Marengo et al., 1997). Within the Bbasin, convection is often organized into squall lines (Cohen et al., 1995) that, frequently occurring as large systems originating at the northern coast and are triggered by local sea breeze circulation (Grecco et al., 19945). Some of these squall lines propagate to Ccentral Amazonas, dissipating during the night and reactivating the next day by diurnal heating.

Climate controls on the Amazon Bbasin rainfall come from episodes of El Niño/La Niña episodes, which are defined by the tropical Pacific Ocean sea surface temperatures (SSTs) and from the tropical Atlantic SSTs (Marengo et al., 2013, 2016). Warm tropical Atlantic SSTs are associated with drought conditions in the Amazon region. During El Niño episodes, most of the Amazon Bbasin experiences below–average rainfall, while during La Niña cases, the basin experiences are associated with above–averagenormal rainfall. The convective activity in most of the Amazon Bbasin is part of the South American Mmonsoon Ssystem (SAMS), which is associated with distinct wet and dry seasons (Silva Dias and Carvalho, 2016).

Horel et al. (1989) used satellite downward longwave radiation to characterized the seasonal variations in the Amazon region and found that the region experiences a, with typical wet and dry seasons each year, withs including two transition periods in between them. Machado et al. (2004) has defined regionally, inside the Amazon basin, the driest month and the duration of the dry season regionally within the Amazon Bbasinduration. The dry season duration varies from only one month in the northwest sector to 3-4 months in southeastern Amazonas. For the Central Amazonas region, July, August and September are typically the driest months. Convection in Amazonas is more intense during the dry to wet transition season, during which when thunderstorms exhibithave more lightning activity (Albrecht et al., 2011) and when they are more sensitive to aerosol loading and topography (Gonçalves et al.and Machado, 20154). TDuring the transition from the dry to the wet season is influenced by complex interactions between smoke-derived aerosols and deep convective clouds occurs (Albrecht et al., 2011). Although the seasonal variability in the average cConvective aAvailable pPotential eEnergy (CAPE) seasonal variability is small, the tail of the CAPE’s seasonal distribution (computed as the surface parcel) seasonal distribution exhibits relatively higher values during the dry to wet season transition than during the wet season (Williams et al., 2002). During the dry season, the aerosols produced by biomass burning in central South America impact a larger area, reaching the tropical Pacific, subtropical South America and South Atlantic (Andreae et al., 2001; Freitas et al., 2005, 2016;, Camponogara et al., 2014).

While the Amazonas region exhibits strong seasonal variations inof atmospheric circulation and related precipitation patterns, the diurnal cycle is typically the same throughout the year. Most of the region has an afternoon peak of convective activity; however, there are selected areas experiencewhere quite intense nocturnal systems are observed and more pronounced where seasonality is more pronounced (Saraiva et al., 2016). The diurnal cycle of convection cycle is has a strongly linked to the underlying surface features (Machado et al., 2004; Silva Dias et al., 2002), including: its topography (Laurent et al., 2002), deforestation (Saad et al., 2010) and large rivers (Dos Santos et al., 2014;, Silva Dias et al., 2004), demonstrating a link to surface features (Machado et al., 2004, Silva Dias et al., 2002). Additionally, large rivers impact rainfall’s the evolution of rainfall through the convergence of the river breezes with ambient air flow (Fitzjarrald et al., 2008). Adams et al. (2016) have shownshowed that one of the climate model’s central problems of the climate model related to the Amazon’s diurnal

convection and rainfall variability ~~of convection and rainfall~~ is the transition from shallow ~~-~~ to ~~-~~ deep convection, which occurs on a time scale of approximately three hours.

The evolution of the boundary layer in the Amazon region has been studied~~,~~ during intensive field observations conducted in different sub-regions in the Amazon Basin, including~~:~~ The Amazon Boundary Layer Experiment (ABLE 2A, 2B, see Harris et al., 1988, 1990), the Anglo-Brazilian Amazonian Climate Observation Study (ABRACOS, see Gash et al., 1996), the Large-Scale Biosphere ~~-~~Atmosphere experiment in Amazonia (LBA, see Silva Dias et al., 2002), the Cloud Processes of the Main Precipitation Systems in Brazil: A Contribution to Cloud-Resolving Modelling and to the Global Precipitation Measurement (CHUVA, Machado et al., 2014) combined with ACRIDICON (Aerosol, Cloud, Precipitation, and Radiation Interactions and Dynamics of Convective Cloud Systems, Wendisch et al., 2016~~7~~), and the Green Ocean Amazon GoAmazon2014/5 (Martin et al., 2017). Fisch et al. (2004) have indicated that the evolution of the boundary layer in the Amazon is linked to land cover and soil moisture, with a deeper mixed layer in the dry season over deforested areas and a shallower mixed layer over forested areas. During the wet season, there are small differences between the evolution of the mixed layer ~~evolution~~ over forested and deforested regions.

During the dry season, the lower atmosphere is polluted by high aerosol concentrations caused by both~~,~~ biomass burning and ~~longer~~prolonged aerosol ~~lifetime~~ suspension associated with~~because of~~ reduced precipitation (Artaxo et al., 2002 and Martin et al., 2010). During the wet season, the atmosphere is mostly clean and convective, and the landscape is referred to as the Green Ocean (Roberts et al., 2001~~;~~, Williams et al., 2002 and Andreae et al., 2004) because the convection there resembles storms over blue oceans, where the warm phase in clouds generally produces rain. Large urban areas, however, introduce perturbations into the pristine air (Martin et al., 2016, 2017).

The complex physico-chemical interactions observed in the Amazon B~~b~~asin include~~s~~ ~~the processes of~~ rainfall formation processes~~;~~, diurnal, seasonal, and interannual ~~annual~~ cycles; the~~, cloud~~ spatial organization of clouds~~;~~, the mechanisms controlling cloud condensation nuclei~~Cloud Condensantion Nuclei~~ (CCN); and~~,~~ the interactions between the vegetation, atmospheric boundary layer, clouds and ~~the~~ upper troposphere. These processes are all in perfect sync~~combination~~, resulting in a stable equilibrium climate that produces rainfall equivalent to 2.3 metres throughout~~along~~ the 6.1 million square kilometres of the Amazon~~as~~ B~~b~~asin, or the equivalent of an average~~to~~ 27 trillion metric tons of rainfall each year ~~on average~~. However, this amazing, complex mechanism can be modified by human activities. ~~Recent results prove~~A recent study illustrates and quantifies~~y~~ (Fu et al., 2013) how this stable environment can be disturbed and the ~~promptly move to another~~ point of equilibrium shifted far from the one that produces abundant fresh water, keeps the forest alive and ~~has a main~~plays a primary role in controlling ~~the~~ global atmospheric~~e~~ circulation and energy distribution.

1.2 Knowledge about Cloud Process in the Amazon Acquired during Field Campaigns

~~In particular, t~~The most recent GoAmazon2014/5, and CHUVA-ACRIDICON measurement campaigns ~~provided Amazonas with~~established a comprehensive dataset to elucidate the complex aerosol-cloud-precipitation interactions within the Amazon

Bbasin. The GoAmazon observations, collected over two years, have delivered a wealth of data ~~to study~~on aerosol-cloud-precipitation (ACP) interactions (Martin et al., 2016). During the two intensive operation periods (IOPs)~~,~~ conducted during the wet and dry seasons, additional airplane data were collected by~~in~~ the IARA (Intensive Airborne Research in Amazonas)~~,~~; Martin et al.~~,~~ (2017) and the ACRIDICON campaign (Wendisch et al., 201~~7~~6). The ~~overall~~ data collected under the umbrella of~~in~~ the ~~framework of~~ GoAmazon campaign also include~~s~~ the CHUVA Pproject (Machado et al., 201~~5~~4) and several other initiatives, which have compiled the most complete dataset in Amazonas ~~to study the~~associated with atmospheric chemical and physical interactions. GoAmazon2014/5 data were collected~~held~~ in the environs of Manaus city, the capital of Amazonas State. Manaus is a city of around two million ~~population~~people located~~,~~ in the middle of Central Amazonas and serves~~, serving~~ as a natural laboratory from which to explore the urban pollution effects on ~~the~~ Amazonas's background environment.

Recent work by Gerken et al. (2015) ~~showed~~ has shown~~a~~ strong enhancement of ozone concentrations close to the surface during storm downdrafts in the central Amazon and ~~discusses~~ suggests that~~the important effect of~~ storm downdrafts bringing higher ozone concentrations from middle-higher altitudes play an important role in enhancing ozone concentrations. The same effect was found by Betts et al. (2002) in~~for~~ the southwest Amazon during LBA. Wang et al. (2016) used airplane (G1)~~, using~~ data ~~from the airplane (G1),~~to describe the mechanism by which ~~for maintaining the~~ aerosol concentrations are maintained in the pristine Amazonian boundary layer. A~~The a~~erosol losses via ~~by~~ precipitation scavenging at the surface are~~is~~ replaced by ~~the~~ storm downdraft fluxes that bring ~~a~~ high concentrations of ~~nano s~~ nanosized particles from the upper atmosphere during precipitation events. These nanoparticles combine with the oxidation products of VOCs (Volatile Organic Compounds) to form CCN at the surface and~~,~~ assist in the formation of clouds. Measurements by the G1 and by HALO (High Altitude and Long-Range Research Aircraft) show a very high concentration of nanoparticles in the upper troposphere, with concentrations up to 65,000 particles per cm^3 (Andreae et al., 2017).

Aerosol~~s~~ particles influence cloud formation. Cecchini et al. (2016) have highlighted the effects of the Manaus aerosol pollution plume on ~~the~~ cloud droplet size distribution during the wet season when only a small sensitivity would be expected. They describe~~d~~ the significant influence of the Manaus pollution plume in reducing the size and increasing the number of cloud droplets as well as the total liquid water content. The ACRIDICON-CHUVA campaign collected ~~in situ~~in situ data during 14 research flights using~~with~~ the HALO research aircraft (Wendisch et al., 2016). The high number~~s~~ of flight hours inside growing cumulus clouds allowed a sensitivity analysis of ~~the~~ aerosol concentrations and of the thermodynamic effects of such concentrations in the warm phase of cumulus clouds. Cecchini et al. (2017a) have also demonstrated that a 100 %~~n~~ increase ~~of 100 %~~ in ~~the~~ aerosol concentrations led to an 84 % increase in the ~~droplet number~~ concentration of droplets, but the same relative increase in vertical velocity corresponded only to a 43 % change. Braga et al. (2017) have compared HALO microphysical probe measurements of cloud droplet ~~number~~ concentrations with a parameterization based on CCN and updraft at the cloud base. Jäkel et al. (2017) have presented a new methodology to retrieve the vertical distribution of the hydrometeor phase using cloud-side reflected solar radiation measurements and have discussed the mixed phase layer as a function of aerosol loading. Giangrande et al. (2016) have presented the statistical behaviour of ~~cloud~~ vertical cloud motions as a function of season, instability and convective inhibition. Burleyson et al. (2016) have discussed the diurnal cycle and spatial variability

Formatado: Sobrescrito

of deep convection among the different GoAmazon sites. Giangrande et al. (2017) have also presented an overview of cloud, thermodynamics, and radiation interactions.

Preceding GoAmazon2014/5, ABLE-2 and LBA collected cloud and rainfall data used to understand the rainfall variability and its interaction with surface vegetation, topography and aerosols in the Amazon. The ABLE-2 project consisted of two expeditions: the first in the Amazonian dry season (ABLE-2A) during Julyly August 1985 and the second, in the wet season (ABLE-2B) during April-May 1987 (Harriss et al., 1988, and 1990). Greco et al. (1990) have described the rainfall and kinematics of the cCentral Amazona using GOES (Geostationary Operational Environmental Satellite) imagery, revealing the importance of the tropical squall lines on the rainfall regime of the Amazonas. Some years later, Garstang et al. (1994), Greco et al. (1994) and Cohen et al. (1995) provided a detailed description of the tropical squall lines in the region. The TRMM-LBA campaign was designed to calibrate the TRMM (Tropical Rainfall Measuring Mission) satellite. The observations were conducted in southern Amazonas, along the arc of deforestation, during the wet season. Several studies contributed to our currentthe understanding of the rainfall variability at different scales. Machado et al. (2002) discussed the complex diurnal cycle interaction at a synopotic scale, while Laurent et al. (2002) examined the mesoscale convective system initiation and propagation;, and Rickenbach et al. (2004) showed the importance of the nocturnal clouds in rainfall in the southwestern Amazonas rainfall. Silva Dias et al. (2002), Petersen et al. (2001), and Cifelli et al. (2002) are some of the studieshave all published findings using TRMM-LBA data to describe the microphysical properties of the rainfall field, the cloud processes, and the biospherice interactions in this region. In addition, different rainfall features have beenwere detected associated with wind regimes; in particular, easterlies and westerlies in the southern Amazon have been associated withto breaks in and active phases of the South American Monsoon System (Silva Dias and Carvalho, 2016, Rickenbach et al et al. 2002). In the nNorthwestern Amazon, northerlies and southerlies are associated with more stratiform and convective systems, respectively (Saraiva et al et al. 20167).

OThere are other studies discussing the rainfall regime in Amazonas State. For example, Tanaka et al. (20145) have described the influence of the river and the city of Manaus in the diurnal cycle of rainfall using based on rain gauge data. Dos Santos et al. (2014) used satellite rainfall products to define the features associated withto the river breezes associated withto the Negro, Solimões and Amazon Rrivers. Fitzgerald et al. (2008) have described the effect of the Tapajos River effect on the rainfall, and Silva Dias et al. (2004) have shown howshowed the wind structure that favours cloud formation on the upwind side of the Tapajós Rriver during daytime. Negri et al. (2000) used passive microwave radiances to construct a 10-year climate related toology of the Amazonas's rainfall patterns. Saraiva et al. (2016) have described the general statistics of the related to Amazonas rainfall using the meteorological S-band radar operational network and have discussed the diurnal cycle as well as the relationship between reflectivity and the cloud electrification process.

All of these studies have contributed to the establishment of oured the basic knowledge about the rainfall statistics and related processes in Amazonas; they have, provideding a new perspective forof research in Amazonas and have elucidateding several aspects of the ACP interactions. The studies associated with field campaigns covered specific seasons (normally the wet season) or resulted from sparse rain gauge or indirect measurement datas with low spatial and temporalce and time resolutions.

In GoAmazon2014/5, the extensive set of rainfall dataset collected usingby the S, X, and W band radars;, airplanes;, disdrometers, vertical pointing radar;, rain gauges;, microwave radiometers;, ceilometers;, and LIDARs provides a comprehensive view of the main variabliliities and characteristics of the precipitation in the cCentral Amazona.

Giangrande et al. (2017) present an overview covering theof clouds aspects that primarily , mainly focuseising on the diurnal cycle and itsthe impact on the radiative effects and thermodynamics effects of clouds. This study presents an overview of the rainfall characteristics and sensitivities to vegetation, topography, and aerosols particles and evaluates the seasonal variability of these factors. The main goal is to discuss the sensitivities of the primarymain processes controlling rainfall over the cCentral Amazon usinga, employing a relatively long time series (2014-2015) of data based on athe comprehensive dataset collected during GoAmazon2014/5 and complemented by aircraft measurements made during ACRIDICON-CHUVA.

Section 2 describes the data and methodology employed in the study. Section 3 presents the results and discussions of the seasonal rainfall characteristics and sensitivities to aerosol, vegetation and topography;, and Section 4 summarizes the major findings.

2. Data and Methodology

Several instruments were employed in this study. This section describes the instruments and the data processing procedures. Figures 1 and 2 in the Martin et al. (2016) study, in the same special issue, show the GoAmazon site locations and the flight tracks of the G-1 aircraft. Wendisch et al. (2016) show the flight tracks (Figure 6) of the HALO aircraft during the ACRIDICON-CHUVA campaign.

A laser precipitation disdrometer (PARSIVEL, see Löffler-Mang and Joss, 2000) measures the size and terminal velocity of hydrometeors that pass through the detection area sampled by a laser beam (54 cm^2) overin a specific time interval. Two different PARSIVEL disdrometers were used during the entire whole campaign: one during thefrom CHUVA Project from January to September 2014 and another duringfrom ARM (Atmospheric Radiation Measurement) from September 2014 to October 2015. Raindrops larger than 5 mm were eliminated from the datasetas to best match the co-located rain gauge accumulated rainfall;, and a complementary filter was applied, as described by Giangrande et al. (2016). The drop size distribution (DSD) and all the respective rainfall rates (RR, in mm h^{-1}) and mean mass-weighted mean diameters (D_m, , in mm) were obtained in 5-minute intervals for periods wherewith RR ≥ 0.5 mm h^{-1}, as suggested by Tokay et al. (2013).

The Doppler radar S-band dataset consists of retrievals from the Manaus radar operated by the Amazon Protection System (SIPAM). The reflectivity and RRrain rate fields were computed using the 2.5 km SIPAM Manaus S-band Constant Altitude Plan Position Indicator (CAPPI) for each radar volume at, every 10- minute intervalss. The corrected radar reflectivity forfrom each volume waswere interpolated to a fixed grid on which the rainfall products were generated. Specific procedures were applied to the dataset to compute RRsrain rates from reflectivity, to reduce noise, and to improve data quality. First, RRsrain rates were computed using a Z-R relationship adjusted to the region using 2014 wet -season impact disdrometer data: $Z=174.8R^{1.56}$. This is a fixed Z-R relationship for convective and stratiform clouds and for both the wet and dry seasons.

Therefore, the total rainfall estimated should be considered ~~as~~ a reference by which to study the differences among the topography and vegetation classes and not as an absolute, precise rainfall amount. The maximum and minimum RR~~rain rate~~s considered were 160 mm h^{-1} and 0.5~~2~~ mm h^{-1}, respectively. The ~~Rain~~RR ~~rate~~ was not computed when the radar beam had less than 10% quality reflectivity values (non-null reflectivity). Finally, a range filter was applied to remove ~~the~~ pixels closer than 10 km and farther than 135 km from the radar.

The Doppler radar X-band dual-polarization dataset was obtained by the mobile Meteor 50DX Selex radar during the CHUVA Project (Schneebeli et al., 2012). The radar data underwent three main processinges ~~steps~~, including differential phase shift (PhiDP) filtering and specific differential phase (KDP) derivation, differential reflectivity (ZDR) offset correction, and horizontal reflectivity (Zh) and ZDR attenuation correction. The uncorrected raw differential phase shift had~~s~~ a noisy signal that ~~needs to be filtered~~required filtering and smoothinged before ~~the calculation of~~ its range derivative (KDP) could be calculated. Several methods ~~can be used~~were available for use, such as a moving average, median filters, and linear programming approaches. In this study, we used the finite impulse response (FIR) filter~~,~~ based on Hubbert and Bringi (1995). Once the filtered PhiDP profile was~~is~~ obtained, KDP was~~is~~ calculated using a least squares linear fit. To verify and calibrate the accuracy of the differential reflectivity measurement, a vertical pointing, rotating scan (also known as "bird-bath" scan) was incorporated into the X-band scan strategy. During light precipitation and in the absence of strong winds, the vertical and horizontal return~~ed~~ signals of a vertical~~ly~~ ly oriented beam should be the same. Differences between the h~~H~~orizontal ~~channels~~ and v~~V~~ertical channels may appear due to poor calibration between the channels, random effects, beam-filling, or side-lobe clutter contamination, among other factors (Gorgucci et al., 1999). Although a~~the~~ standard calibration was performed, careful examination of the ZDR behaviour before and after the calibration~~se changes~~ was necessary. We selected all of the observations with no radar gates higher than 30 dBZ below 2 km and analysed the overall ZDR values and ~~the~~ temporal changes in the mean value. A persistent, positive ZDR offset (approximately 0.5 dB) was~~were~~ found and applied to the data. After these steps, we applied an~~the~~ attenuation correction. X-band radars are more prone to signal attenuation due to rain than C- and S-band radars. It is therefore mandatory to correct the signal for attenuation prior to any analysis using reflectivity data, if such a correction is possible (Schneebeli et al., 2012). With a dual-polarization system, one can use the differential phase shift to calculate the attenuation due to rain. We applied the ZPHI method (Testud et al., 2000) to the entire~~whole~~ dataset where dual-polarization moments were available. The corrected Zh and ZDR values were then ready to be used as inputs for~~to~~ rainfall analyse~~i~~s or hydrometeor classification studies.

The cloud droplet size distributions were derived from the HALO measurements using a cloud droplet probe (CDP, Lance et al., 2010; Molleker et al., 2014 and Wendisch and Brenguier, 2013). This instrument measures the droplet size distribution within the size range of 3 µm to 50 µm based on the hydrometeor's forward scattering properties. The DSD is sorted into 15 size bins for each measurement cycle. The probe was operated at a 1 Hz frequency. The major sources of uncertainty for~~of~~ the instrument are as follows (Weigel et al., 2016): (a) uncertainty in the cross-section area (0.278 mm^2 +/- 15%), (b) the relatively small sample volume (cross-sectional area multiplied by aircraft speed), and (c) counting statistics for each size bin. As noted by Molleker et al. (2014), the CDP uncertainty is approximately 10 %. Braga et al. (2017) performed an ~~inter~~comparison

between the CDP and the other HALO cloud probes and concluded that they agree within instrumental uncertainties. The vertical wind component (w) was measured by the Basic HALO Measurement and Sensor System (BAHAMAS) located at the nose of the aircraft (Wendisch et al., 2016) and calibrated according to Mallaun et al. (2015). The uncertainty in w is approximately 0.3 m s^{-1}.

Using the disdrometer or the CDP, the ~~mean~~ mass-weighted mean diameter (D_m) was computed as the ratio between the fourth and third moments (liquid water content) of the DSD (see Bringi et al., ~~D_m~~ 2002 for a detailed description). For every five minutes of a continuous rainfall event (defined as RR ≥ 0.5 mm h^{-1}), the moments were computed using a parameterization derived by Tokay and Short (1996) ~~parameterization~~.

A condensation particle counter (CPC, TSI 3010) in the Aerosol Observing system instruments from ARM measured the ~~number~~ concentration of individual aerosol particles at 10 m above ground level at the T3 site ~~,~~(main GoAmazon site at Manacapuru, see Martin et al., 2016 for a detailed description). The data were~~was~~ averaged to ~~a~~ five ~~-~~ minute~~s time~~ interval~~s~~ covering the period from January 2014 to March 2015 (Thalman et al., 2017). B~~The b~~ackground or polluted conditions were defined based on the specific CPC distribution for each season~~,~~ by the threshold value associated with the 33% and 66% percentile~~,~~ respectively, for the dry and wet season~~s~~. The threshold values and details are presented in the relevant~~specific~~ section~~s below~~.

The total ~~number~~ concentration of individual cloud condensation nuclei particles (N_{CCN}(S)) was measured with a continuous-flow stream wise thermal-gradient CCN counter (model CCN-200, DMT, Longmont, CO, USA) (Rose et al., 2008). The measured aerosol was sampled by the HALO aerosol submicrometer inlet (HASI)~~. P~~. P~~a~~rticles with a critical supersaturation (S=0.52 ± 0.05 %) were~~are~~ activated and form~~ed~~ water droplets. Water droplets with a diameter ≥ 1 µm were~~are~~ detected by an optical particle counter. Details about the measurement mode can be found in~~by~~ Andreae et al. (2017). The error in supersaturation resulted from the calibration uncertainty, as described by M. Pöhlker et al. (2016); it is estimated to be in the range of 10%.

This study considers the wet and dry seasons as the months of January to March and August to October~~,~~ respectively. Some instruments ~~only~~ operated only during the two GoAmazon2014/5 IOPs: IOP1~~,~~ during the wet season~~,~~ and IOP2 during the dry season~~. IOP1,~~ correspond~~sing~~ to February to March and IOP2 to 15 September to 15 October~~, respectively~~. The S-band radar data ~~is~~ are available for both years (2014 and 2015), while the X-band ~~only~~ operated only in the 2014 IOPs.

Thermodynamic~~s~~ parameters such as CAPE, Convective Inhibition Energy (CINE), Precipitable Water Vapour (PWV), Lifting Condensation Level (LCL) and bulk shear were computed using the T3 radiosondes at 00, 06, 12 and 18 UTC for 2014. The thermodynamic~~s~~ parameters were computed using temperature and humidity at the surface. Bulk shear is defined as the difference between the average surface-6 km wind velocity and the surface-500 m wind velocity.

3. Results and Discussion

This section first discusses the rainfall characteristics and variability by comparing the wet and dry seasons to establish the primarymain differences between seasons. Section 3.2 discusses the studies of sensitivity analyses relativeies to aerosols, vegetation and topography.

3.1 Rainfall Seasonal Variability

SThe seasonal variability will be presentedwas analysed from different perspectives, including general patterns, regional differences, characteristics of the observations from satellite (clouds) and radar (rainfall) observation characteristics, the DSDdrop size distribution, rainfall vertical profile, and hydrometeor populations.

3.1.1 General Precipitation and Thermodynamic Patterns.

Amazonas has a distinct seasonal variability with distinctguished wet and dry seasons. The length and start date of the definitions of wet season length and beginning depends on the region location within the Amazonas Basin. The mean monthly rainfall (2014-2015) for the wet season was 369 mm for the wet season (considering a month of 30 days) and only 87 mm for the dry season. These numbers show the large difference expected between the two seasons. However, from the the RRrain rate point of view (considering only when is raining) also exhibited, the seasonality also presents differences. The mean RRrain rate (computed in 5 minutes intervals) for the wet season was 7.7 mm h^{-1}, while that for the dry season wascompared to 9.4 mm h^{-1} for the dry season. Therefore, although the dry season has approximately 4 times less accumulated rainfall was recorded during the dry season than the wet season, the average rainfall event during the dry season produced a greater amount of rain has a higher rain rate. Figure 1 reveals this feature, where the relative rainfall rate distribution for the wet season shows higher relative frequency for RR < 20 mm h^{-1}, than that of the dry season. On the other hand, the dry season shows higher relative frequency for RR> 20 mm h^{-1}. There was only one event during the wet seasons in which awith record RRrain rate of approximately 100 mm h^{-1} was recorded within a few minutes only. T. The relative population intensity of the dry season rainfall events is more pronounced towards high RR than that of events during the wet season. This distinctive feature has important consequences for the cloud microphysical and macrophysical structures of clouds. The main reason for this difference is associated with the instability and cloud cover. Figure 2 presents monthly box plots for the of the monthly statistics of thermodynamics variables, with the lower (Q1) and upper (Q3) bounds representingare the 25% and 75 percentiles. The whiskers arewere defined by Q1 - 1.5 * IQR (lower) and Q1 + 1.5 * IQR (upper);, IQR is the interquartile range (Q3-Q1).

Figure 2A shows the CAPE distribution for the wet and dry seasons in 2014. The dry season has a larger CAPE than the wet seasonone, and the frequency with which the of CAPE exceedsing 2000 J kg^{-1} is higher during the dry season. The wet season has typical monsoonal rainfall, with widespread moderate rain, in contrast to the more isolated and intense rainfall events that occur during the dry season. Zhuang et al.'s (2017) study ofing shallow-to-deep convection transition in Amazonas found similar results.

This characteristic of rainfall events with where a higher RRrain rate occurs during the dry season rainfall events is explained based onby the seasonal differences in the thermodynamic parameters. Comparing these seasons, important differences can be

~~clearly noted in Fig.~~Figure 2 highlights some of these important differences. The dry season has a larger CAPE, higher CINE, less available water vapour, a higher cloud base, and higher shear than the wet season. The CAPE increases from March to September; and the largest tail distributions occur at the end of the year when humidity increases and cloud base decreases. During the dry season, only regions with strong forcing can produce convective clouds that~~to~~ use the higher CAPE and shear available to produce organized convection. Gonçalves et al. (2015~~4~~) show that ~~the higher~~increased RR~~rain rate~~s (radar reflectivity values larger than 35 dBZ) during the dry season mainly occur~~s~~ over ~~the higher topography~~higher elevations in Amazonas (section 3.2.1). The higher CINE and~~,~~ smaller amount of water vapour reduces the occurrence of convection, but when convection is able to~~can~~ develop, it has all the ingredients to be deeper. Machado et al. (2004) explain~~s~~ that the more intense convective clouds during the dry to wet season transition may result from less ~~"~~competition~~"~~ of surface moisture convergence to feed cumulonimbus clouds because ~~there is~~ a smaller number of rain cells exist. Figure 2f presents the RR~~rain rate~~ statistics for 2014 and the monthly rainfall measured by rain gauge in T3.

3.1.2 Size Distribution of Cloud Clusters and Rain Cells

Cloud clusters and rain cell ~~calculations were computed using the~~data were derived from GOES-13 satellite images and S-band radar ~~employing~~ using the ~~algorithm called~~ Fortracc (Forecasting and Tracking Cloud Clusters see Vila et al., 2008) algorithm. A cloud cluster is defined by connected ensembles of pixels with brightness temperatures (BT)~~,~~ for ~~channel~~ the 10.5 µm channel that are~~,~~ colder than 235 K, as defined by Machado et al. (1988). A r~~R~~ain cell~~s~~ is defined as a connected ensemble~~s~~ of pixels in the radar 2.5 km CAPPI with reflectivity larger than 20 dBZ. ~~Embedded in the cloud clusters, q~~Quite often, rain cells, which are embedded in cloud clusters, are observed when clouds start to form~~have~~ raindrops. ~~Considering the wet and dry seasons, the typical~~The average cloud cluster size and lifespan are~~have~~ 75-km effective radius (hereafter called ~~as~~ radius) and ~~a~~ 1.5 ~~-~~hour~~s~~, respectively, during the wet and dry seasons in the Amazon. The typical rain cell ~~size~~ has a 7.5-km radius and a~~n~~ 0.6-hour lifespan. On average, cloud clusters are 10 times larger and have lifespans of~~times~~ approximately three times that of their associated ~~the~~ rain cells. These are ~~the~~ average characteristics; ~~and, there is a wide range of~~ cloud cluster~~s~~ come in a wide range of sizes. Cloud clusters can ~~have more than a~~exceed 300 ~~-~~km in radius and have a lifespan~~time~~ longer than 24 h~~ours~~, while rain cells can grow to ~~sizes occur~~ up to approximately 60 ~~-~~km in radius and ~~lifetime of a~~last for a couple of hours. Figure 3 shows the dry and wet season cloud cluster~~s~~ and rain cell size distributions identified in this study, as well as~~and~~ the differences between~~among~~ them. The basic size distribution ~~is not very different~~does not vary substantially between the two seasons because cloud cluster size distribution ~~has a power law~~follows an exponential ~~size~~ distribution, as shown by Machado et al. (1992); however, certain distinctions~~, but some clear characteristics~~ can be noted if the difference is computed. The wet season has more small and large rain cells and cloud clusters than the dry season. The dry season produces more rain cells in the range of a 10-km radius and cloud clusters of an approximately 40-km radius. The ratio between the cloud cluster and rain cell average radii during the wet season is much ~~higher~~ greater because of the larger stratiform cloud decks typical of a monsoon cloud regime. The thermodynamics of the dry season environment discussed in the preceding section favour~~s~~ the organization

of more compact and active convection~~,~~ with more intense rainfall events ~~rates~~ but ~~with an~~ accumulated rainfall amounts that are 4 times smaller.

3.1.3 Mass-Weighted Mean Rainfall ~~Mean Mass-Weighted~~ Diameter for the Dry and Wet Seasons

~~An important aspect to be evaluated is related to the different~~ Variations in cloud processes between the two Amazonian seasons were evaluated in this study in order to determine whether~~. Are there~~ important microphysical differences between raindrops during~~in~~ the wet and dry seasons exist, or whether~~are~~ only ~~the~~ RR~~rain rate~~ and rainfall frequency vary between seasons.~~different? The way to investigate t~~These features were investigated through the~~included the~~ deployment of disdrometers and a dual-polarimetric radar. ~~It is important to consider that t~~This study focuses on rainfall and raindrops~~;~~ however,~~ and that~~ seasonal differences in cloud droplet size distributions may warrant attention as well~~be quite different~~.

For instance, the effect of ~~the~~ aerosol concentrations on ~~the~~ cloud droplets~~,~~ in shallow convective clouds, where aerosols generally reduce~~ing~~ the size and increase~~ing~~ the concentration of~~for~~ a given liquid water content, is well known (Cecchini et al., 2016, among several other studies). However, if a polluted cloud transitions from shallow ~~-~~ to ~~-~~ deep convection, aerosols can invigorate clouds (Rosenfeld et al., 2008~~;~~~~,~~ Koren et al., 2012~~;~~~~,~~ Gonçalves et al., 2015~~4~~). Giangrande et al.~~,~~ (2017) present~~ed~~ the G1 airplane cloud particle distribution measurements taken during GoAmazon2014/5 and~~,~~ show~~ing~~ the predominance of larger cloud droplets~~,~~ in warm clouds during~~, in~~ the wet season. The ~~in situ~~in situ cloud droplet data were collected for a shallow cloud population. The result is very different when ~~the comparison among~~ seasonal data collected~~s is made~~ using disdrometers that measure raindrops at least 100 times larger ~~(in their mean~~ measured as mass-weighted mean diameter (D_m)) are compared. Given that~~As the~~ raindrop diameter depends on ~~the~~ RR~~rain rate~~, which varies~~is different~~ between the two seasons, ~~the comparison between~~ dry and wet season D_m values ~~for the dry and wet seasons~~ were compared~~performed~~ as a function of ~~the~~ RR~~rain rate~~ in 5 mm h^{-1} intervals. ~~Another important feature to be evaluated in the comparison is the d~~Different frequencies of convective and stratiform clouds during~~in~~ the wet and dry seasons also merit evaluation. As discussed by Giangrande et al. (2017), ~~the wet season has higher occurrence of~~ stratiform clouds occur more often in the wet season than the dry season; hence, ~~the~~ D_m ~~evaluation~~ should be ~~performed~~ evaluated separately for convective and stratiform clouds. The cloud classification employed in this study was ~~computed~~ performed using the radar wind profiler (RWP) and ancillary data as described by Giangrande et al. (2017) from March 2014 to December 2015. Clouds were classified based on the predominant cloud type in the warm cloud layer. Convective clouds include strong and weak convection, while stratiform clouds include those ~~the classification of the stratiform~~ with and without a well-defined bright band~~ and stratiform with a not well defined bright band~~.

Figures 4a and 4b show the D_m for the wet and dry seasons as functions of the RR~~rain rate~~ for convective and stratiform clouds. The arrows on the x-axis mark distributions where the averages ~~are different~~vary given~~, with~~ a statistical significance of 95%. For convective clouds, ~~it is clear that~~ the ~~mean~~ mass-weighted mean diameter is larger during the dry season for a given RR~~rain rate~~. This result suggests the different cloud processes generate~~ing~~ larger rainfall drops. The differences in shallow clouds

during the dry season may be due to the reduced humidity, as shown in Figure 2c, which can reduce supersaturation and increase droplet evaporation via entrainment. However, if a cloud evolves into the deep convective stage, the higher cloud base, shear, and CAPE induce stronger vertical motions and mesoscale organization, generating higher quantities of ice (shown in next section) and forming larger raindrops through melting of large ice particles such as snow and graupel. For stratiform clouds (Figure 4b), the difference between the two seasons is much smaller and significant only for very lowsmall RRsrain rates.

3.1.4 Cloud Vertical Profiles for the Dry and Wet Seasons

The results presented above discuss the rainfall at the surface levelon the ground. In order toTo comprehensively better understand the cloud processes associated with the dry and wet seasons includes the evaluation ofwe must evaluate the hydrometeor vertical profiles of precipitating clouds. AnThe X-band dual-polarization radar was installed atin the T3 site and operated during the two GoAmazon2014/5 IOPS in February-March and September-October 2014. To account for potentialavoid wet radome attenuation effects and obtain usefulgood dual-polarization measurements with sufficientgood vertical coverage, the data analysed to build the next figures included only cases without rain over the radar and for data collected within the 10- and 60-km radius range. Based in the radar strategyAs described in the data methodology section, the volume scan was processed with attenuation correction and a ZDR offset to build the contoured frequency by altitude diagrams (CFAD) for the dry and wet seasons for theof reflectivity (Z), specific differential phase (KDP), differential reflectivity (ZDR), and the horizontal and vertical correlation coefficient that measuresfor the consistency of the H and V returned power and phase offor each pulse for both the wet and dry seasons.

Figure 5 shows the reflectivity CFAD for the dry and wetwet and dry seasons. One can note theThe typical stratiform and convective patterns for the wet and dry seasons are clearly visible, respectively. For the wet season, the bright band is very clear and haswith a pronounced peak of reflectivity at approximately at 4 km, which corresponds to the layer where ice is meltsing and increasing the reflectivity increases. Moreover, the upper levels above the melting layer have less intense reflectivity, demonstrating the less intense convective process that occurs in the majority of cases during the wet season. For the dry season, the typical convective profile with a higher reflectivity in the lower levels corroborates the higher RRsrain rates observed during this season. In addition, the mixed and glaciated layers exhibithave a more frequent occurrence of high reflectivity values, indicating the presence of large ice hydrometeors.

Figure 6 shows the CFAD for the dual-polarization parameters, ZDR, KDP and co-polar correlation coefficient. The hydrometeor response to the transmitted signal depends on several factors that can change the may alter certain characteristics of the measured signal, such as hydrometeor orientation by the electrification field (see Mattos et al., 2017 for a detailed discussion), ice density, and different crystal shapes. Of course, there are also other possible effects that may impact the data quality, such as resonance and partial beam-filling. Although the CFADs are not completely different, as given that these parameters have a small range of variation and are subject to the limitations described above, some clear differences among

the seasonsseasonal differences can be observed. The ZDR that mostly describes the largely reflects ice orientation containshas a larger frequencygreater number of near-zero or negative signals duringin the dry season than duringcompared to the wet season. This can be is likely associated with the crystal orientation by the electrical field, as more lightning occurs the dry season has much more lighting than the wet season (see Williams et al., 2002) and morepossibly ice vertically ly oriented ice shapes such as graupel may occur during the dry season than the wet season. The KDP distribution shows considerably larger values in the warm layer, in during the dry compared to thewith wet season, indicating that the higher RRsrain rates and greater numberhigher frequency of positive values in the mixed phase areis probably associated with intense updrafts, as shown by Giangrande et al., (2016). The correlation coefficient highlights an interesting feature. During the dry season, it seems that there appears to beis a clearer distinction between the mixed phase and the glaciation phase above 8 km. The wet season correlation coefficient is more homogenous with height inside the cloud. Cecchini et al. (2017b) and Jakel et al. (2017) discuss the greaterlarger efficiency of clouds forming in a clean environment to produce ice. The dry season exhibitspresents average higher average correlations at approximately 8 km, demonstrating a deeper and unmixed water layer of water at these heights. This feature canlikely indicates that clouds forming during the wet season have a smaller mixed phase than the clouds forming during the dry season and under poor air quality conditions in a much more polluted environment.

3.2 Rainfall Sensitives to Aerosols, Topography, and Vegetation

This section presentsstudies the rainfall sensitivities to different surface types, topography and aerosol number concentrations. Ancillary data describing vegetation type, topography and aerosol concentrations, as well as measurements from the HALO airplane, are employed to study the total rainfall, RRrain rate, cloud droplet and raindrop sensitivities to these environmental and geographical characteristics.

3.2.1 Rainfall D_m as a Function of Rainfall Rateain Rate for Polluted and Clean Cases

The impact of the aerosol number concentration on the cloud microphysical properties needs to be analysed for the different seasons. Particle concentrations measured at the surface using the CPC, at the surface, for during the dry and wet seasons are very differentvary greatly from one another. For instance, the 33rd and 66th percentiles are 673 cm-3 and 1377 cm-3 for the wet season and are 1954 cm-3 and 3392 cm-3 for the dry season, respectively. The dry season has nNearly three times as many more aerosols are present during the dry compared to than the wet season, which can have strong substantial implications for cloud and rainfall formation. However, as shown in Figure. 2, the thermodynamic characteristics are also very differentvary greatly, and the differences cannot be explained only by the difference in aerosol concentrations difference. To evaluate the impact of aerosols impact on cloud processes, the rainfall mean mass-weighted mean rainfall diameter must beis evaluated for different population of particle concentrations duringfor each season. However, after analysis, thisthe comparison was possible only possible duringfor the wet season because the rainfall events with particle concentrations exceeding 66th percentile in the

dry season ~~for the cases with particle concentrations exceeding 66th percentile~~ were rare. During the dry season, the upper one-third of ~~the population of~~ aerosol concentrations ~~is~~ are characterized mostly by drier days. The d~~D~~ry season is characterized by biomass burning and ~~with around 6~~approximately 6 times more ~~aerosols~~ mass ~~-~~ loaded~~ing~~ (organic) aerosols than~~that~~ during the wet season.~~,~~ Shilling et al. (2018) describe~~s~~ the typical aerosol types~~species~~ and the evolution of organic aerosol particles during the wet and dry season in the Manaus pollution plume. Figure 7 shows the D_m during the wet season for background (particle concentrations less than the 33rd percentile) and polluted (particle concentrations greater ~~more~~ than the 66th percentile) conditions as a function of RR~~rain rate~~. This calculation requires two different instruments to be co-located. Therefore, the number of samples from~~population of~~ each 5 ~~-~~ minute~~s~~ continuous rainfall event intervals~~s~~, in each RR~~rain rate~~ class was drastically reduced. Consequently, the differences between the two air quality categories~~populations~~ in each RR~~rain rate~~ bin were significant only at the 85% level. Even if the differences between the two average values for background and polluted cases are not significant, the physical results show clear trends~~are coherent~~. For low~~small~~ RRs~~rain rates~~, which are more often associated with warm cloud processes, the cases with background aerosol concentrations have a larger D_m because there are fewer CCN and lower cloud droplet concentrations, resulting in large raindrops. However, for greater~~higher~~ RRs~~rain rates~~, which are typically associated with deep convection, the D_m is greater~~higher~~ for polluted clouds, demonstrating the major effect of convective invigoration discussed in the preceding section. Rosenfeld and Ulbrich (2003) used~~ing~~ satellite data to estimated~~ the~~ raindrop size distributions for continental and maritime Amazon clouds (LBA). They found that c~~C~~louds over the continent produce~~s~~ greater concentrations of large drops and smaller concentrations of small drops. They suggested that this behaviour is caused by the effects of aerosols ~~effects~~ on ~~the~~ precipitation formation~~ing~~ processes.

3.2.2 Rainfall Sensitivity to Surface Cover

There is a very complex diurnal cycle over the Amazonas basin. Burleyson et al. (2016) used 15 years of satellite data to show a heterogeneous spatial distribution of convection that results from numerous local effects of ~~the~~ rivers and vegetation cover. Using radar data, Saraiva et al. (2016)~~, using radar data,~~ also found the Amazonas diurnal cycle to vary~~be~~ regionally ~~varying~~. In addition to the natural geographic~~al~~ effect, ~~there is~~ rainfall modulation occurs through~~by~~ anthropogenic-induced changes in vegetation and ~~by~~ the presence of large cities. ~~Laurent~~ Durieux et al. (2003) ~~showed the differing~~have shown that cloud cover varies as a function of the deforestation pattern. Lin et al. (2010), among several other studies, have discussed the urban heat island effect on the region's climate. To understand how vegetation cover influences ~~the~~ precipitation characteristics, two approaches were applied~~studied~~: one using statistical radar data and the other~~another~~ using a special HALO mission specifically aimed at this topic.

For the statistical approach, the RR~~rain rate~~ was calculated from the SIPAM S-band radar data~~was employed to compute the rain rate~~ for the dry and wet seasons, as described in Section 2. S~~The s~~urface cover was obtained from the digital Terra-Class classification data (Almeida et al., 2008). This database ~~presents~~ contains 15 vegetation classes~~, of vegetation~~ such as forest; hydrology; urban areas; and several ~~classes of~~ deforestation classes, ~~including~~,including clean and dirty pasture, deforested

areas, and exposed soil, among others. These classes were regrouped in four ~~specific classes~~categories for this study: forest (covering 76.9% of the studied region), hydrography (16.3%), non-forest (6.2%), and urban area (0.5%). These two ~~sets of~~ data~~sets~~ were combined to evaluate the different RRs~~rain rates~~ for each surface cover type. Terra-Class has 300 m resolution and was interpolated to the radar grid ~~considering~~ using the most frequent surface type class. Figure 8 presents the spatial distribution of the vegetation classes (Fig~~ure.~~ 8a) over the 150 km radius of the S~~-~~band radar and the topography of the region (Fig~~ure.~~ 8b).

Figure 9 shows the RR~~rain rate~~ box plot~~s statistics~~ for each surface type in the wet and dry seasons. This analysis does not consider cloud life cycle or the different thermodynamic or dynamic~~s~~ conditions that may have been present ~~or the cloud life cycle. It~~ and only considers ~~the overall~~those statistics present among the different surface types. The different behaviours are a consequence of different physical processes~~, in~~ which will be discussed in this section.

For the wet season, the RR~~rain rate statistics vary~~varies little among the different surface cover classes. However, for the dry season, ~~one can note differences such as~~ a ~~higher~~ greater amount of rainfall occurred over the urban areas and smaller amounts occurred over non-forested regions. ~~As expected, i~~In general, the dry season RR~~rain rate~~ was greater~~is higher~~ than that in the wet season. The median and ~~the~~ tail of the distribution were~~are~~ larger over urban areas and smaller over deforested areas. The ~~median values~~ difference between the median values of non-forested and urban RRs~~rain rates~~ in ~~for~~ the dry season was~~is~~ approximately 25%. Although the ~~statistical population of~~number of radar pixels in each class ~~are very different~~varied and the urban area represents only 0.5% of the area, the box plot patterns are different~~.~~. The smaller differences during the wet season can be~~are~~ expected because~~as the~~ rainfall during this season~~, as described above,~~ has a strong ~~component of~~ stratiform cloud component~~s~~ typical of a monsoon rainfall regime, as described above. In this type of regime~~, the~~ large-scale dynamic forcing is very strong, and ~~the~~ surface type has little impact. However, during the dry season, rainfall events largely depend on local forcing and surface latent heat flux. Manaus, as an urban centre, is characterized by a strong heat island effect (Souza and Alvala, 2014~~2~~) that creates a convergence fed by moisture from the surrounding forest. The non-forested area has less available latent heating than the forest, which may~~might~~ contribute to lower RRs~~rain rates~~. ~~We should clarify that t~~These ~~are the~~ results are associated with~~for the~~ RR~~rain rate~~ and not ~~for the~~ total rainfall ~~amount~~data. T~~The t~~otal rainfall ~~amount~~ is larger over the forest and hydrology areas (not shown).

Fisch et al. (2004) have discussed the differences in the boundary layer between forest and pasture. They show, for the Amazonas dry season, that the height of the fully developed convective boundary layer over forest is approximately 1100 m, and it is approximately 50% higher over pasture. During the wet season, the forest and pasture have nearly the same boundary layer height (approximately 1000 m). Does the different thermodynamic behaviour during the dry season result in different cloud microphysical properties and, consequently, different radiative forcing? This is a very important question because climate change simulations in Amazonas need to correctly reproduce the cloud processes over~~in~~ each of these surface covers. The results presented above consider ~~the~~ RR~~rain rate~~ and the ~~final effect~~impacts of the surface on ~~the~~ cloud~~s~~. Several physical processes play an important role in the generation of the different RRs~~rain rates~~ between different surface types, such as the ~~different~~ boundary layers described above. The effect of ~~the~~ surface type on ~~the~~ cloud droplet distribution under~~on the~~ shallow

convection conditions is not well ~~elaborated~~understood. One of the ACRIDICON-CHUVA HALO missions was especially designed to investigate this relationship~~feature~~. ~~One could consider that the c~~Cloud processes for different surface covers may~~could~~ be evaluated from a statistical point of view as a function of the surface cover using~~with~~ a combination of data from several different flights~~' data from a statistical point of view as a function of the surface cover~~. However, airplane flights are limited to a few hours and ~~the flights~~ measure ~~the~~ clouds for different meteorological conditions, heights, thermodynamic conditions, and aerosol loadings that, as already stated in the set of papers published using the GoAmazon data, have a strong impact on cloud microphysical properties. Therefore, a specific flight mission was designed to evaluate this matter. The ~~flight~~ AC17 flight, which was completed on 27 September 2014, ~~was a mission~~ look~~ed~~ing at the ~~cloud~~ contrast between clouds above forest and pasture surfaces. The objectives were to observe and compare ~~clouds~~ macrophysical and microphysical cloud properties over both forest and pasture areas under~~at~~ comparable environmental conditions. As the flight legs occurred at the same fixed level, the thermodynamics and aerosol concentrations were nearly the same due to the short flight time and path ~~(, only~~ 40 km~~),~~, in each region. The two flight ~~-~~leg paths are shown in Figure 10. C~~The c~~loud profiling was carried out over ~~the 80 km~~both 40-km legs (red lines in Figure~~.~~ 10), which included~~are~~ forested, transition, and pasture surface covers~~areas~~. The flight plan for the cloud profiling legs was designed for a fixed altitude~~s~~ level for~~in~~ each leg in order to profile clouds along~~during~~ the trajectories. The flight level was selected as a function of the cloud development at the local time for each flight leg. Leg 1 occurred at 1500 UTC (11:00 LST) and leg 2 at 1700 UTC (13:00 LST). The height of the flights employed in this study were 1500 m, 1900 m and 2500 m. In leg 2, the cloud base was higher and the clouds were measured at 1900 m and 2500 m. In Figure 10, the GOES visible image shows the increase in~~of~~ cloud cover from the first flight to the second, as well as ~~and~~ the typical shallow cumulus clouds measured. During t~~T~~he morning leg 1 flight, ~~in the morning,~~ the cloud base was~~were~~ nearly the same over both the forested and non-forested areas;~~,~~ however, during the ~~flight in the~~ afternoon flight, the cloud base over the non-forested area appeared to ~~could~~ be slightly higher than that over the forested area. Therefore, some differences among clouds can also be related to ~~the~~ measurements taken at the same height but in a different cloud layer.

~~The analyses were performed using~~Only 350 seconds of measurements from~~in~~ each region and at each flight level were used in this analysis. ~~In this way,~~Data from the beginning of the flight over the forest, the boundary between the forested and ~~-~~deforested region, and the final flight path over the deforested region were discarded so that~~, and~~ only data from the centres of the forested and deforested regions were evaluated. Figure 11a shows a scatter plot of the cloud droplet ~~number~~ concentration and liquid water content for flight leg 1 over the forest and pasture at ~~around 1~~approximately 1500 m, 1900 m and 2500 m. ~~There is~~~~This data~~ These data show~~s~~ a nearly linear relationship, with a correlation coefficient ~~correlation~~ ranging ~~between~~ from 0.94 to 0.99 ~~between~~ for the relationship between cloud droplet ~~number~~ concentration and liquid water content ~~among the different~~at varying heights. For~~At~~ a fixed cloud droplet ~~number~~ concentration, clouds over the forested area have more liquid water than clouds over pasture at the same height. This means cloud droplets that develop~~ing~~ over ~~the~~ rain forests are larger than those that evolve~~ing~~ over pastures. Therefore, ~~the~~ cloud droplet size distribution is different between the two regions, with forested areas producing larger cloud droplets.

Figure 12 shows the cumulative histogram of the CCN ~~number~~ concentrations (N_{CCN}) for the two legs over the forested and non-forested regions at ~~around 1~~approximately 1500, 1900 and 250~~00m~~ m. The decrease in~~of~~ N_{CCN} with ~~the~~ altitude for boundary layer aerosols agrees with~~to~~ the other flights carried out during the ACRIDICON-CHUVA campaign, as shown in Andreae et al. (2017). The magnitude of the N_{CCN} is typical for polluted regions in Brazil~~,~~ and falls~~means in~~ between strong biomass burning events and forested regions far away~~off~~ from biomass burning events. For l~~L~~eg 1, N_{CCN} distribution is nearly identical at the~~for~~ 1500 and ~~also in~~ 1900 m flight heights for ~~at~~ both the forested and~~/~~ non-forest regions~~;~~, however at~~for~~ 2500 m, the distributions are quite different, with the~~while~~ non-forested region exhibiting a greater ~~has larger~~ N_{CCN}. For l~~L~~eg 2, the difference between the two surface types is larger, and the non-forested regions exhibited~~present~~ higher N_{CCN} than the~~over~~ forested region at ~~for~~ all altitudes. In the first leg, the difference between forested and deforested regions increased with ~~the~~ altitude, and the deforested regions ~~always have more~~exhibited greater N_{CCN}.~~:~~ Two factors should be considered: leg 1 occurred~~s at~~ ~~around 1~~approximately 11:00 LST~~;~~, therefore, the convective boundary layer was not fully developed, and at 2500 m, the measurements likely represent ~~probably~~ the residual boundary layer from the previous day. Leg 2~~,~~ occurred later, at ~~around 1~~approximately 13:00 LST, when the boundary layer was deeper and well mixed. Another important factor ~~to be considered~~ is the regional wind direction from east~~; , therefore,~~ for leg 1, the air over the forest was the air advected from the deforested region, and for leg 2, a north-south transect flight, the air was advected from the homogenous forest along~~at~~ the easterly side.

The cloud microphysics differences between the forested and deforested clouds are probably related to these~~this~~ differences in the N_{CCN} distributions. ~~One can note that s~~Some clouds over pastures have the same ~~amount of~~ liquid water quantities as clouds over forests~~,~~; although the pasture clouds contained~~have~~ higher cloud droplet ~~s number~~ concentrations. This could result from several processes, such as larger vertical motion induced by the higher sensible heating~~, and/or~~ by the large aerosol concentration over pasture and/or the high-water availability over the forest.

Figures 11b and 11c show the D_m and cloud droplet ~~number~~ concentrations as a function of ~~the~~ vertical motion. ~~It is clear in t~~These figures illustrate that the larger cloud droplet diameter samples ~~population~~ over the forest and the larger cloud droplet ~~s number~~ concentrations increase~~ing~~ with ~~the~~ vertical velocity (updraft and downdraft), but there is not a clear relationship between vertical velocity and D_m. V~~The v~~ertical velocity increases supersaturation but does not appear to modulate ~~the~~ droplet size. Cecchini et al. (2017a) also found that different flights ~~to have~~demonstrated a small correlation between ~~the~~ vertical motion and droplet size. Nevertheless, ~~the~~ cloud droplet concentrations are more ~~is better~~ linearly related to ~~the~~ vertical motion (correlation coefficient is ~~correlation are around 0~~approximately 0.6). The stronger the updrafts are, the higher the ~~number~~ droplet concentration ~~is~~. This relationship does not appear to show differences between forested and pasture areas.

3.2.3 Rainfall Sensitivity to Topography

The topography database employed in this study included~~was~~ the digital elevation data from ~~the~~ NASA Shuttle Radar Topographic Mission and has a~~with~~ resolution of 90 m at the equator (Jarvis et al., 2008). Figure 8 shows the topographic~~y~~

spatial distribution within~~inside~~ the 150 km radius of the radar's coverage. As the sample size~~data population~~ decrease~~d~~s logarithmically relative to~~as the~~ elevation increases, the classes were binned in log intervals as follows: from 0 to 15 m, from 15 to 40 m, from 40 to 83 m and from 83 to 157 m. Using the S-band radar data, a statistical box plot was constructed~~built~~ for each topography class (Figure 13). For the wet season, ~~one can note that~~ the statistics are nearly the same for all topography classes. The highest topography class shows nearly the same median but a slightly smaller tail distribution. However, for the dry season, considerable ~~box plot~~ differences are found among the topography classes. The higher the land surface~~topography is~~, the longer~~higher is~~ the ~~tail of the~~ RR~~rain rate~~ distribution tail. During the dry season, convective inhibition is higher, as shown in Figure~~.~~ 2, and ~~the~~ cloud formation requires some kind of forcing to overcome this inhibition and take advantage of the higher CAPE available during this season. Topography is one ~~of the~~ forcing mechanism that allows this to occur, even if the differences are only a few hundred metres.

4. Summary and Conclusions

The Amazonas climate is comprised of~~entails~~ distinctive and complex interactions between~~among~~ a multitude of different physical processes that~~,~~ result~~ing~~ in one of the most important rainfall production systems on Earth. ~~The i~~Interannual variability is high, and in recent years, the~~records of~~ driest and wettest years on record have been observed. El Niño, La Niña, and ~~the~~ Atlantic Ocean temperatures are some of the interannual features affecting ~~the~~ total rainfall. ~~Alternatively~~In addition, ~~there are~~ many synoptic conditions affect ~~responsible for the~~ large-scale rainfall mechanisms. These are the ingredients necessary to generate large amounts of rainfall in Amazonas, and they are normally organized in mesoscale convective systems. C~~The c~~loud and precipitation systems differ during~~in~~ the wet and dry seasons. ~~The t~~Total ~~amount of~~ rainfall in the wet season is 4.2 times larger than that in the dry season, but ~~the dry season~~ RRs~~rain rates~~ observed during the dry season are ~~is~~ approximately 22% higher than those that occur~~that~~ in the wet season. The wet season has a smaller CAPE, CINE, vertical wind shear, and cloud base height and a greater~~larger~~ amount of integrated water vapour than the dry season. The wet season typically has monsoon-type rainfall, while convection occurs at a smaller scale during the dry season ~~convection is organized at a smaller scale than in the wet season~~. The typical cloud cluster in Amazonas (wet and dry season) has an effective radius of approximately 75 km and a 1.5-hour life cycle. The rain cells inside these cloud clusters have an average radius of approximately 7.5 km and a~~n~~ 0.6-hour life cycle. ~~The s~~Seasonality also modulates the size distribution of these features. The wet season has more small and large cloud clusters and rain cells, which are typical of isolated cumuliform convection and monsoon rainfall cloud organization. The dry season has proportionally more cloud clusters and rain cells of approximately 40 km and 10 km radii, respectively, favouring a cloud organization that is reduced in size but larger than that of isolated convection. The differences between the two seasons are also observed in the ~~clouds~~' microphysics of the clouds. ~~During the dry season, r~~Rainfall drops are larger in convective clouds during the dry season than during the wet season, likely~~, for the convective clouds probably~~ due to enhanced ice processes. For stratiform clouds, larger drops are also observed~~,~~ but are not statistically significantly different.

The cloud hydrometeor vertical profile signature was evaluated for the first time in Amazonas in this study. X-band dual-polarization radar data werewas used to provide dual-polarization CFAD variables for the dry and wet seasons. As expected, there are differences between the dual-polarization statistical distributions between the seasons. The wet season cloud type has a typical bright band at approximately 4 km altitude. The dry season has a stronger reflectivity below and above the melting layer, which is characteristic of the liquid water and ice profiles of stronger convective clouds. The ZDR profile ofin the dry season indicates more vertically-ly-oriented ice, while the KDP profile revealedpresented larger positive values in the mixed phase, consistent with more frequent and stronger updrafts. During the dry season, the correlation coefficient indicated more inhomogeneous heterogeneous clouds above the melting layer, with two distinct layers above and below under 8-km height. This indicates a clearer characterization of the mixed phase and glaciation layers.

The evaluation of the effect of aerosol number concentrations on the raindrop size distribution shows an interesting feature. Due to the small statistical sample of rainfall events during the dry season for different ranges of aerosol loadings, it was only possible to evaluate the aerosol effect during the wet season. Clean cases show larger raindrops for lower RRsrain rates, and polluted cases show larger raindrops for a higher RRsrain rates. For a RRrain rate less than 8 mm h^{-1}, the typical warm rain and less organized convective rainfall events, the clean cases have a more straightforward interpretation based on the small number of CCN and consequently larger droplets. However, when convection becomes deeper with increasedlarger RRsrain rates, the polluted cases seem to invigorate convection, as suggested by Rosenfeld et al. (2008).

General statistics for howthe surface type impactsing the RRrain rate werehad significant results only for the dry season. The wet season had nodid not exhibit different RRsrain rates for different surface types. For the dry season, urban regions had the highest RRrain rate, and deforested regions had the lowest. This is probably related to the Manaus heat island effect, with moisture provided by the surrounding forested area and the smaller latent heating fluxes in large deforested areas, respectively. Nearly identicalsimultaneous cloud properties were measured by the HALO airplane over the forested and deforested areas. The specific flight design, which allowed for an evaluation of to evaluate the microphysical differences in shallow convective cloud formation, provided unprecedented data to study thesethis differences under with nearly the same synoptic and environmental conditions. Nearly simultaneous flight legs at the same height, alongin a short pathpatch of only 40 km, allowed us to compare the cloud processes over different surfaces types. As a result, it was observed that clouds over forested areas were observed to have larger cloud droplets, and in general, the vertical velocity wasis well correlated with the cloud droplet number concentrations. However, these data did not it is uncorrelated with mass-weighted mean the cloud droplet mean mass-weighted diameter.

Finally, the impact of topography impact on the RRrain rate was evaluated. There was no difference in the RRrain rate during the wet season for different topography classes. For the dry season, there was a clear increase in the RRrain rate as elevationthe topography increased. This was probably related to the topographicaly forcing required to overcome the large CINE and take advantage of the large CAPE available during this season.

The results presented indicate that the GoAmazon data set brings new insights into the process of cloud and rainfall formation in the Amazon, and to and to those complexities requiringthat need further research. There isis the entire dataset is likely to

have a very high potential impact ~~of the whole data set into~~on the modelling of aerosol, cloud, and landscape features in tropical scenarios. Nevertheless, there are several ~~fruitful~~ areas that still necessitate further~~for potential future~~ research to complete the ~~full~~ picture of ~~the~~ cloud processes in Amazonas. For instance, a~~the~~ detailed microphysical description of clouds as a function of the two patterns of convection, ~~the~~ cumuliform and deep convection~~.~~, is still wanting (see Wang et al., 2018). C~~The c~~hanges in the microphysical properties and mixed phase are some of the unknown behaviours of cloud processes. How these processes change as function of the season, cloud life cycle, aerosol loading, and topography are some examples of areas in need of ~~that need to have~~ further research~~studies~~ to improve the cloud modelling over continental tropical regions. Another potential area for future ~~detailed~~ study includes~~ies is~~ the implications and solutions for GCMs, which ~~that~~ may not resolve ~~such~~ subtle variations in topography but are~~and is~~ very important in ~~for to~~ trigger~~ing~~ convection during the dry season.

Acknowledgements: We thank all participants in the GoAmazon2014/5 and ACRIDICON-CHUVA for their ~~great~~ cooperation and for making~~, which made~~ this study possible. We acknowledge FAPESP (São Paulo Research Foundation) Projects 2009/15235-8, 2014/08615-7 and 2015/14497-0. This work was conducted under scientific licenses 001030/2012-4, 001262/2012-2 and 00254/2013-9 of the Brazilian National Council for Scientific and Technological Development (CNPq). Institutional support was provided by the Central Office of the Large-Scale Biosphere Atmosphere Experiment in Amazonia (LBA), the National Institute of Amazonian Research (INPA), the National Institute for Space Research (INPE), ~~and~~ Amazonas State University (UEA), and the Brazil Space Agency (AEB). We acknowledge the support of ~~the ACRIDICON-CHUVA campaign by~~ the Max Planck Society, the German Aerospace Centre~~r~~ (DLR), and the German Science Foundation (Deutsche Forschungsgemeinschaft, DFG) within the DFG Priority Program SPP 1294 for the ACRIDICON-CHUVA campaign. We also acknowledge the Atmospheric Radiation Measurement (ARM) Climate Research Facility, a user facility of the U.S. DOE, Office of Science, sponsored by the Office of Biological and Environmental Research, and support from the ASR program. J. Fan was supported by the Climate Model Development and Validation program funded by the Office of Biological and Environmental Research in the US Department of Energy Office of Science. R. Albrecht was supported by CNPq 459546/2014-7. We acknowledge Dr. Y. Zhuang and anonymous reviewers for their comments and suggestions.

References

Adams, Adams, D. K., Barbosa, H. M. J., and De Los Rios, K. P. C.: A spatiotemporal water vapor/deep convection correlation metric derived from the Amazon Dense GNSS Meteorological Network, Monthly Weather Review, http://dx.doi.org/10.1175/MWR-D-16-0140.1, 2016.

Albrecht, R. I., Morales, C. A., and Silva Dias, M. A. F.: Electrification of precipitating systems over the Amazon: Physical processes of thunderstorm development, Journal of Geophysical Research, 116, D08209, doi:10.1029/2010JD014756, 2011.

Almeida, C.A., Coutinho, A.C., Esquerdo, J.C.D.M., Adami, M., Venturieri, A., Diniz, C.G., Dessay, N., Durieux, L., and Gomes, A.R.: High spatial resolution land use and land cover mapping of the Brazilian Legal Amazon in 2008 using Landsat-5/TM and MODIS data, In: Acta Amazonica, 46(3), 291-302, http://www.inpe.br/cra/projetos_pesquisas/dados_terraclass.php, 2016.

Andreae, M. O., Artaxo, P., Fischer, H., Freitas, S. R., Lelieveld, J., Dias, M. A. F. S., Freitas, S., and Longo, K. M., Strom, J.: Transport of biomass burning smoke to the upper troposphere by deep convection in the equatorial region, Journal of Geophysical Research, 28(6), 951-954, 2001.

Andreae, M.O., Rosenfeld, D., Artaxo, P., Costa, A. A., Frank, G. P., Longo, K. M., and Silva Dias, M. A.: Smoking rain clouds over the Amazon. Science, 303, 1337-1342, 2004.

Andreae, M. O., Afchine, A., Albrecht, R., Holanda, B. A., Artaxo, P., Barbosa, H. M. J., Bormann, S., Cecchini, M. A., Costa, A., Dollner, M., Fütterer, D., Järvinen, E., Jurkat, T., Klimach, T., Konemann, T., Knote, C., Krämer, M., Krisna, T., Machado, L. A. T., Mertes, S., Minikin, A., Pöhlker, C., Pöhlker, M. L., Pöschl, U., Rosenfeld, D., Sauer, D., Schlager, H., Schnaiter, M., Schneider, J., Schulz, C., Spanu, A., Sperling, V. B., Voigt, C., Walser, A., Wang, J., Weinzierl, B., Wendisch, M., and Ziereis, H.: Aerosol characteristics and particle production in the upper troposphere over the Amazon Basin, Atmos. Chem. Phys. Discuss., https://doi.org/10.5194/acp-2017-694, in review, 2017.

Artaxo, P, Martins, J. V. , Yamasoe, M. A. , Procópio, A. S. , Pauliquevis, T. M. , Andreae, M. O. , Guyon, P. , Gatti, L. V., and Leal, A. M. C.: Physical and chemical properties of aerosols in the wet and dry season in Rondonia, Amazonia, Journal of Geophysical Research, 107, 8081-8095, 2002.

Betts, A. K., L. V. Gatti, Cordova, A. M., and Silva Dias, M. A. F., Fuentes, J. D.: Transport of ozone to the surface by convective downdrafts at night, Journal of Geophysical Research, 107, 1–13, 2002.

Braga, R. C., Rosenfeld, D., Weigel, R., Jurkat, T., Andreae, M. O., Wendisch, M., Pöhlker, M. L., Klimach, T., Pöschl, U., Pöhlker, C., Voigt, C., Mahnke, C., Borrmann, S., Albrecht, R. I., Molleker, S., Vila, D. A., Machado, L. A. T., and Artaxo, P.: Comparing parameterized versus measured microphysical properties of tropical convective cloud bases during the ACRIDICON–CHUVA campaign, Atmos. Chem. Phys., 17, 7365-7386, https://doi.org/10.5194/acp-17-7365-2017, 2017.

Bringi, V. N., Huang, G.-J., Chandrasekar, V., and Gorgucci, E.: A methodology for estimating the parameters of a gamma raindrop size distribution model from polarimetric radar data: Application to a squall-line event from the TRMM/Brazil campaign, J. Atmos. Oceanic Technol., 19, 633–645, 2002.

Burleyson, C., Feng, Z., Hagos, S., Fast, J., Machado, L., and Martin, S.: Spatial Variability of the Background Diurnal Cycle of Deep Convection around the GoAmazon2014/5 Field Campaign Sites, J. Appl. Meteorol. Clim., 55, 1579–1598, doi:10.1175/JAMC-D-15-0229.1, 2016.

Camponogara, G., Silva Dias, M. A. F., and Carrió, G. G.: Relationship between Amazon biomass burning aerosols and rainfall over the La Plata Basin, Atmos. Chem. Phys., 14, 4397-4407, 2014.

Cavalcanti, I. F. A., Ferreira, N. J., and Silva, M. G. A. J. (Eds.): Weather and Climate in Brazil (Tempo e Clima no Brasil - in Portuguese), Oficina Texto, 463, 2009.

Cecchini, M. A., Machado, L. A. T., Comstock, J. M., Mei, F., Wang, J., Fan, J., Tomlinson, J. M., Schmid, B., Albrecht, R., Martin, S. T., and Artaxo, P.: Impacts of the Manaus pollution plume on the microphysical properties of Amazonian warm-phase clouds in the wet season, Atmos. Chem. Phys., 16, 7029-7041, https://doi.org/10.5194/acp-16-7029-2016, 2016.

Cecchini, M. A., Machado, L. A. T., Andreae, M. O., Martin, S. T., Albrecht, R. I., Artaxo, P., Barbosa, H. M. J., Borrmann, S., Fütterer, D., Jurkat, T., Mahnke, C., Minikin, A., Molleker, S., Pöhlker, M. L., Pöschl, U., Rosenfeld, D., Voigt, C., Weinzierl, B., and Wendisch, M.: Sensitivities of Amazonian clouds to aerosols and updraft speed, Atmos. Chem. Phys., 17, 10037-10050, https://doi.org/10.5194/acp-17-10037-2017, 2017a.

Cecchini, M. A., Machado, L. A. T., Wendisch, M., Costa, A., Krämer, M., Andreae, M. O., Afchine, A., Albrecht, R. I., Artaxo, P., Borrmann, S., Fütterer, D., Klimach, T., Mahnke, C., Martin, S. T., Minikin, A., Molleker, S., Pardo, L. H., Pöhlker, C., Pöhlker, M. L., Pöschl, U., Rosenfeld, D., and Weinzierl, B.: Illustration of microphysical processes in Amazonian deep convective clouds in the Gamma phase space: Introduction and potential applications, Atmos. Chem. Phys. Discuss., https://doi.org/10.5194/acp-2017-185, in review, 2017b.

Cifelli, R., Petersen, W. A., Carey, L. D., Rutledge, S. A., and Silva Dias, M. A. F.: Radar observations of kinematic, microphysical, and precipitation characteristics of two MCSs in TRMM-LBA, Journal of Geophysical Research, 107, doi:10.1029/2000JD000264, 2002.

Cohen, J. C. P., Silva Dias, M. A. F., and Nobre, C. A.: Environmental conditions associated with Amazonian squall lines: A case study. Monthly Weather Review, 123, 3163-3174, 1995.

Diedhiou, A., Machado, L. A. T., and Laurent, H.: Mean kinematic characteristics of synoptic easterly disturbances over the Atlantic, Advances in Atmospheric Sciences, 27, 483–499, 2010.

Dos Santos, M.J.; Silva Dias, M.A.F.; and Freitas, E.D.: Influence of local circulations on wind, moisture, and precipitation close to Manaus City, Amazon Region, Brazil, J. Geophys. Res. Atmospheres, 119, 233–249, doi:10.1002/2014JD021969, 2014.

Fisch, G., Tota, J., Machado, L. A. T., Silva Dias, M. A. F., Lyra, R. F., Nobre, C. A., Dolman, A. J., and Gash, J. H. C.: The convective boundary layer over pasture and forest in Amazonia, Theor. Appl. Climatol. 78, 47–59, doi:10.1007/s00704-004-0043-x, 2004.

Formatado: Português (Brasil)

Fitzjarrald, D. R., Sakai, R. K., Moraes, O. L. L., Oliveira, R. C., Acevedo, O. C., Czikowsky, M. J., and Beldini, T.: Spatial and temporal rainfall variability near the Amazon–Tapajós confluence, J. Geophys. Res., 113, G00B11, doi:10.1029/2007JG000596, 2008.

Freitas, S. R., Longo, K. M., Silva Dias, M., Silva Dias, P., Chatfield, R., Prins, E., Artaxo, P., Grell, G., and Recuero, F.: Monitoring the transport of biomass burning emissions in South America, Environmental Fluid Mechanics, 5, 135–167, doi:10.1007/s10652-005-0243-7, 2005.

Fu, R., Yin, L., Li, W., Arias, P.A., Dickinson, R.E., Huang, L., Chakraborty, S., Fernandes, K., Liebmann, B., Fisher, R., Myneni, R.B,. Increased dry-season length over southern Amazonia in recent decades and its implication for future climate projection. Proceedings of the National Academy of Sciences 110, 18110–18115. doi: 10.1073/pnas.1302584110, 2013.

Freitas, S.R., Panetta, J., Longo, K. M., Rodrigues, L. F., Moreira, D. S., Rosário, N. E., Silva Dias, P. L., Silva Dias, M. A. F., Souza, E. P., Freitas, E. D., Longo, M., Frassoni, A., Fazenda, A. L., Santos e Silva, C. M., Pavani, C. A. B., Eiras, D., França, D. A., Massaru, D., Silva, F. B., Cavalcante, F., Pereira, G., Camponogara, G., Ferrada, Gonzalo A., Campos Velho, H. F., Menezes, I., Freire, J. L., Alonso, M. F., Gácita, M. S., Zarzur, M., Fonseca, R. M., Lima, R. S., Siqueira, R. A., Braz, R., Tomita, S., Oliveira, V., Martins, L. D.: The Brazilian developments on the Regional Atmospheric Modeling System (BRAMS 5.2): an integrated environmental model tuned for tropical areas, Geoscientific Model Development Discussions, 130, 1-55, 2016.

Garstang, M., Massie, H. L., Halverson, Jr. J., Greco, S., and Scala, J.: Amazon coastal squall lines. Part 1: Structure and kinematics, Monthly Weather Review, 122, 608-622, 1994.

Gash, J. H. C., Nobre, A., Roberts, J. M., and Victoria, R. L. (Eds.): An overview of ABRACOS, in Amazon Deforestation and Climate, John Wiley, New York, 1996.

Gerken, T., Wei, D., Chase, R. J., Fuentes, J. D., Schumacher, C., Machado, L. A. T., Andreoli, R. V., Chamecki, M., Souza, R. A. F., Freire, L. S., Jardine, A. B., Manzi, A. O., Santos, R. M. N., Randow, C. V., Costa, P. S., Stoy, P. C., Tóta, J., and Trowbridge, A. M.: Downward transport of ozone rich air and implications for atmospheric chemistry in the Amazon rainforest, Atmos. Environ. Part A, 124, 64–76, doi:10.1016/j.atmosenv.2015.11.014, 2015.

Giangrande, S. E., Toto, T., Jensen, M. P., Bartholomew, M. J., Feng, Z., Protat, A. and Machado, L. A. T.: Convective cloud vertical velocity and mass-flux characteristics from radar wind profiler observations during GoAmazon2014/5, J. Geophys. Res. Atmos., 121, 891–913, doi:10.1002/2016JD025303, 2016.

Giangrande, S. E., Feng, Z., Jensen, M. P., Comstock, J., Johnson, K. L., Toto, T., Wang, M., Burleyson, C., Mei, F., Machado, L. A. T., Manzi, A., Xie, S., Tang, S., Silva Dias, M. A. F., de Souza, R. A. F., Schumacher, C., and Martin, S. T.: Cloud Characteristics, Thermodynamic Controls and Radiative Impacts During the Observations and Modeling of the Green Ocean Amazon (GoAmazon2014/5) Experiment, Atmos. Chem. Phys. Discuss., https://doi.org/10.5194/acp-2017-452, in review, 2017.

Gonçalves, W. A., Machado, L. A. T., and Kirstetter, P.-E.: Influence of biomass aerosol on precipitation over the Central Amazon: an observational study, Atmos. Chem. Phys., 15, 6789-6800, https://doi.org/10.5194/acp-15-6789-2015, 2015.

Formatado: Português (Brasil)

Gorgucci, E., Scarchilli, G., and Chandrasekar, V.: A procedure to calibrate multiparameter weather radar using properties of the rain medium, IEEE T. Geosci. Remote, 37, 269–276, 1999.

Greco, S., Swap, R., Garstang, M., Ulanski, S., Shipham, M., Harriss, R. C., Talbot, R., Andreae, M. O., and Artaxo, P.: Rainfall and surface kinematic conditions over central Amazonia during ABLE 2B, J. Geophys. Res., 95, 1-14, 1990.

Greco, S., Scala, J., Halverson, J., Massie, H. L., Jr., Tao-K, W., and Garstang, M.: Amazon coastal squall lines. Part II: Heat and moisture transports, Monthly Weather Review, 122, 623-635, 1994.

Harriss, R. C., Wofsy, S. C., Garstang, M., Browell, E. V., Molion, L. C. B., McNeal, R. J., Hoell, J. M., Bendura, R. J., Beck, S. M., Navarro, R. L., Riley, J. T., Snell, R. L.: The Amazon Boundary Layer Experiment (ABLE-2A): Dry season 1985, J. Geophys. Res., 93, 1351–1360, 1988.

Harriss, R. C., Garstang, M., Wofsy, S. C., Beck, S. M., Bendura, R. J., Coelho, J. R. B., Drewry, J. W., Hoell, J. M., Matson, Jr., P. A., McNeal, R. J., Molion, L. C. B., Navarro, R. L., Rabine, V., and Snell, R. L.: The Amazon Boundary Layer Experiment: Wet season 1987, J. Geophys. Res., 95, 721-736, 1990.

Horel, J., Hahmann, A., and Geisler, J.: An investigation of the annual cycle of the convective activity over the tropical Americas, Journal of Climate, 2, 1388–1403, 1989.

Hubbert, J. and Bringi, V.N.: An iterative filtering technique for the analysis of copolar differential phase and dual-frequency radar measurements, J. Atmos. Oceanic Technol., 12, 643-648, 1995.

Jäkel, E., Wendisch, M., Krisna, T. C., Ewald, F., Kölling, T., Jurkat, T., Voigt, C., Cecchini, M. A., Machado, L. A. T., Afchine, A., Costa, A., Krämer, M., Andreae, M. O., Pöschl, U., Rosenfeld, D., and Yuan, T.: Vertical distribution of the particle phase in tropical deep convective clouds as derived from cloud-side reflected solar radiation measurements, Atmos. Chem. Phys., 17, 9049-9066, https://doi.org/10.5194/acp-17-9049-2017, 2017.

Jarvis, A., Reuter, H.I., Nelson, A., and Guevara, E.: Hole-filled SRTM for the globe Version 4, available from the CGIAR-CSI SRTM 90m Database, “available at: http://srtm.csi.cgiar.org”, 2008.

Koren, I., Altaratz, O., Remer, L. A., Feingold, G., Martins, J. V., and Heiblum, R. H.: Aerosol-induced intensification of rain from the tropics to the mid-latitudes, Nat. Geosci., 5, 118–122, doi:10.1038/ngeo1364., 2012.

Kousky, V. E., and Gan, M. A.: Upper tropospheric cyclonic vortices in the tropical South Atlantic, Tellus, 33, 538-551, 1981.

Lance, S., Brock, C. A., Rogers, D., Gordon, J. A.: Water droplet calibration of the Cloud Droplet Probe (CDP) and inflight performance in liquid, ice and mixed-phase clouds during ARCPAC, Atmos. Meas. Tech., 3, 1683-1706, doi:10.5194/amt-3-1683-2010, 2010.

Durieux, L., Machado, L.A.T., and Laurent, H.: The impact of deforestation on cloud cover over the Amazon arc of deforestation, Remote Sens. Environ., 86, 132-140, 2003.

Laurent, H., Machado, L. A. T., Morales, C. A., and Durieux, L.: Characteristics of the Amazonian mesoscale convective systems observed from satellite and radar during the WETAMC/LBA experiment, J. Geophys. Res., 107, doi:10.1029/2001JD000337, 2002.

Lin, C. Y., Chen, W. C., Chang, P. L., and Sheng, Y. F.: Impact of the urban heat island effect on precipitation over a complex geographic environment in northern Taiwan, Journal of Applied Meteorology and Climatology, 50, 339-353, 2010.

Löffler-Mang, M., Joss, J.: An optical disdrometer for measuring size and velocity of hydrometeors, J. Atmos. Ocean. Technol. 17 , 130–139, 2004.

Machado, L. A. T., Desbois, M., Duvel, J. P.: Structural Characteristics of Deep Convective Systems over Tropical Africa and the Atlantic Ocean, Monthly Weather Review, 120, 392-406, 1992.

Machado, L. A. T., Laurent, H., and Lima, A. A.: Diurnal march of the convection observed during TRMM-WETAMC/LBA, Journal of Geophysical Research, 107, doi:10.1029/2001JD000338, 2002.

Machado, L. A. T.,H. Laurent, N. Dessay and I. Miranda.: Seasonal and diurnal variability of convection over the Amazonia: A comparison of different vegetation types and large scale forcing, Theoretical and Applied Climatology, 78, doi:10.1007/s00704-004-0043-x, 2004.

Machado, L. A. T., Rossow, W., Guedes, R. L., and Walker, A.: Life cycle variations of mesoescale convective systems over the Americas, Monthly Weather Review, 126, 1630–1654, 1998.

Machado L. A. T, and Coauthors: The CHUVA Project – how does convection vary across Brazil?, Bull. Amer. Meteor. Soc., 95, 1–10, doi: 10.1175/BAMS-D-13-00084.1, 2014.

Mallaun, C., Giez, A., and Baumann, R.: Calibration of 3-D wind measurements on a single-engine research aircraft, Atmos. Meas. Tech., 8(8), 3177–3196, doi:10.5194/amt-8-3177-2015, 2015.

Marengo, J., Cornejo, A., Satymurty, P., Nobre, C., and Sea, W.: Cold surges in tropical and extratropical South America: The strong event in June 1994, Monthly Weather Review, 125, 2759–2786, 1997.

Marengo, J. A., Borma, L. S., Rodriguez, D. A., Pinho, P., Soares, W. R., and Alves, L. M.: Recent Extremes of Drought and Flooding in Amazonia: Vulnerabilities and Human Adaptation, American Journal of Climate Change, 02, 87-96, 2013.

Marengo, J.A, Williams, E.R., Alves, L. M, Soares, W. R., Rodrigues, D. A. (Eds.): Exteme seasonal variations in the Amazon Basin: droughts and floods, In Interaction between biosphere, atmosphere and human land use in the Amazon basin. Nagy, L. Forsberg, B. R., Artaxo, P., eds, Springer, 55-76, 2016.

Martin, S. T., Andreae, M. O., Artaxo, P., Baumgardner, D., Chen, Q., Goldstein, A. H., Guenther, A., Heald, C. L., Mayol-Bracero, O. L., McMurry, P. H., Pauliquevis, T., Pöschl, U., Prather, K. A., Roberts, G. C., Saleska, S. R., Dias, M. A. S., Spracklen, D., Swietlicki, E., and Trebs, I., Sources and properties of Amazonian aerosol particles: Rev. Geophys., 48, RG2002, doi:10.1029/2008RG000280, 2010.

Martin, S. T., Artaxo, P.; Machado, L. A. T.; Manzi, A. O.; Souza, R. A. F.; Schumacher, C.; Wang, J.; Andreae, M. O.; Barbosa, H. M. J.; Fan, J.; Fisch, G.; Goldstein, A. H.; Guenther, A.; Jimenez, J. L.; Poschl, U.; Silva Dias, M. A.; Smith, J. N.; and Wendisch, M.: Introduction: Observations and Modeling of the Green Ocean Amazon (GoAmazon2014/5), Atmospheric Chemistry and Physics (Online), 16, 4785-4797, 2016.

Martin, S. T and Coauthors: The Green Ocean Amazon Experiment (GoAmazon2014/5) Observes Pollution Affecting Gases, Aerosols, Clouds, and Rainfall over the Rain Forest, Bull. Am. Meteorol. Soc., 98, 981-997, doi:10.1175/BAMS-D-15-00221.1, 2017

Mattos, E. V., Machado, L. A. T. , Williams, E. R. , Goodman, S. J. , Blakeslee, R. J. , Bailey, J.: Electrification Life Cycle of Incipient Thunderstorms. Journal of Geophysical Research: Atmospheres, 122, 4670-4697, 2017.

Molleker, S., Borrmann, S., Schlager, H., Luo, B., Frey, W., Klingebiel, M., Weigel, R., Ebert, M., Mitev, V., Matthey, R., Woiwode, W., Oelhaf, H., Dörnbrack, A., Stratmann, G., Grooß, J.-U., Gün-ther, G., Vogel, B., Müller, R., Krämer, M., Meyer, J., and Cairo, F.: Microphysical properties of syn-optic scale polar stratospheric clouds: in situ measurements of unexpectedly large HNO3 containing particles in the Arctic vortex, Atmos. Chem. Phys., 14, 10785-10801, doi:10.5194/acp-14-10785-2014, 2014.

Negri, A. J., Anagnostou, E. N., and Adler, R. F.: A 10-yr climatology of Amazonian rainfall derived from passive microwave satellite observations, J. Appl. Meteor., 39, 42–56, doi:10.1175/1520-0450(2000)039,0042:AYCOAR.2.0.CO;2, 2000.

Petersen, W.A., and Rutledge, S.A.: Regional Variability in Tropical Convection: Observations from TRMM, J. Climate, 14, 3566-3585, 2001.

Pöhlker, M. L., Pöhlker, C., Klimach, T., Hrabe de Angelis, I., Barbosa, H. M. J., Brito, J., Carbone, S., Cheng, Y., Chi, X., Ditas, F., Ditz, R., Gunthe, S. S., Kesselmeier, J., Könemann, T., Lavrič, J. V., Martin, S. T., Moran-Zuloaga, D., Rose, D., Saturno, J., Su, H., Thalman, R., Walter, D., Wang, J., Wolff, S., Artaxo, P., Andreae, M. O., and Pöschl, U.: Long-term observations of cloud condensation nuclei in the Amazon rain forest – Part 1: Aerosol size distribution, hygroscopicity, and new model parameterizations for CCN prediction, Atmos. Chem. Phys., 16, 15709-15740, 10.5194/acp-2016-519, 2016

Rickenbach, T. M.: Nocturnal cloud systems and the diurnal variation of clouds and rainfall in southwestern Amazonia, Mon.Wea. Rev., 132, 1201–1219, doi:10.1175/1520-0493(2004)132,1201, 2004.

Rickenbach, T., Ferreira, R. N., Halverson, J., and Silva Dias, M. A. F.: Modulation of convection in the southwestern Amazon basin by extratropical stationary fronts, J. Geophys. Res., 107, doi:10.1029/2000JD000263, 2002.

Roberts, G. C., Andreae, M. O., Zhou, J., and Artaxo, P.: Cloud condensation nuclei in the Amazon Basin: "Marine" conditions over a continent?, Geophys. Res. Lett., 28, 2807-2810, 2001.

Rose, D., Gunthe, S. S., Mikhailov, E., Frank, G. P., Dusek, U., Andreae, M. O., and Poeschl, U.: Calibration and measurement uncertainties of a continuous-flow cloud condensation nuclei counter (DMT-CCNC): CCN activation of ammonium sulfate and sodium chloride aerosol particles in theory and experiment, Atmospheric Chemistry and Physics, 8, 1153-1179, 2008

Rosenfeld D. and Ulbrich, C. W. (Eds.): Cloud microphysical properties, processes, and rainfall estimation opportunities, Chapter 10 of " Radar and Atmospheric Science: A Collection of Essays in Honor of David Atlas", Edited by Roger M. Wakimoto and Ramesh Srivastava, Meteorological Monographs 52, 237-258, AMS, 2003.

Rosenfeld, D.: Flood or drought: How do aerosols affect precipitation?, Science, 321, 1309–1313, 2008.

Saad, S. I., da Rocha, H. R., Silva Dias, M. A. F., and Rosolem, R.: Can the Deforestation Breeze Change the Rainfall in Amazonia? A Case Study for the BR-163 Highway Region, Earth Interactions, 14, 1-25, 2010.

Santos, M. J., Silva Dias, M.A. F., and Freitas, E. D.: Influence of local circulations on wind moisture and precipitation close to Manaus City, Amazon Region – Brazil, Journal of Geophysical Research, 119, 233-249, doi:10.1002/2014JD021969, 2014.

Saraiva, I., Silva Dias, M. A. F., Morales, C. A. R., and Saraiva, J. M. B.: Regional variability of rainclouds in the Amazon basin seen by a network of weather radars, Journal of Applied Meteorology and Climatology, https://doi.org/10.1175/JAMC-D-15-0183.1, 2016.

Shilling, J. E., Pekour, M. S., Fortner, E. C., Artaxo, P., de Sá, S., Hubbe, J. M., Longo, K. M., Machado, L. A. T., Martin, S. T., Springston, S. R., Tomlinson, J., and Wang, J.: Aircraft Observations of Aerosol in the Manaus Urban Plume and Surrounding Tropical Forest during GoAmazon 2014/15, Atmos. Chem. Phys. Discuss., https://doi.org/10.5194/acp-2018-193, in review, 2018.

Schneebeli, M. , Sakuragi, J. , Biscaro, T. S. , Angelis, C. F. , Costa, I. C. , Morales, C. , Baldini, L. , Machado, L. A. T.: Polarimetric X-band weather radar measurements in the tropics: radome and rain attenuation correction, Atmospheric Measurement Techniques, 5, 2183-2199, 2012.

Silva Dias, M.A. F., and Carvalho, L. M. V. (Eds.): The South American Monsoon System. In: The Global Monsoon System Research and Forecast (3rd Edition) C. P. Chang Ed., World Scientific Publishing Co., Chapter 3. (in press), 2016.

Silva Dias, P. L., Schubert, W. H., and DeMaria, M.: Large-scale response of the tropical atmosphere to transient forcing, J. Atmos. Sci., 40, 2689-2707, 1983.

Silva Dias, M.A.F., Rutledge, S., Kabat, P., Silva Dias , P. L., Nobre, C. A., Fisch, G., Dolman, A J, Zipser, E., Garstang, M., Manzi, A. O., Fuentes, J., Rocha, H. R., Marengo, Jose, Plana-Fattori, A., Sá, L., Alvalá, R., Andreae, M., Artaxo, Paulo, Gielow, R., and Gatti, L.: Clouds and rain processes in a biosphere atmosphere interaction context in the Amazon Region, Journal of Geophysical Research., 107, 46.1 - 46.23, 2002.

Silva Dias, M. A. F., Silva Dias, P. L., Longo, M., Fitzjarrald, D. R., and Denning, A. S.: River breeze circulation in Eastern Amazon: observations and modeling results, Theoretical and Applied Climatology, 78, 111-121, 2004.

~~05 - Siqueira and Machado, 2004:~~

Siqueira, J. R., and Machado, L. A. T.: Influence of frontal systems on the day-to-day convection variability over South America, J. Climate, 17, 1754–1766, 2004.

Souza, D. O. and Alvalá, R. C. S.: Observational evidence of the urban heat island of Manaus City, Brazil, Met. Apps., 21, 186–193, doi:10.1002/met.1340, 2014.

Tanaka, L., Satiamurty, P., and Machado, L. A. T.: Diurnal variation of precipitation in central Amazon Basin, International Journal of Climatology, 34, 2014.

Testud, J., Bouar, E. L., Obligis, E., and Ali-Mehenni, M.: The rain-profiling algorithm applied to polarimetric weather radar data, J. Atmos. Ocean. Tech., 17, 332–356, 2000.

Thalman, R., de Sá, S. S., Palm, B. B., Barbosa, H. M. J., Pöhlker, M. L., Alexander, M. L., Brito, J., Carbone, S., Castillo, P., Day, D. A., Kuang, C., Manzi, A., Ng, N. L., Sedlacek III, A. J., Souza, R., Springston, S., Watson, T., Pöhlker, C., Pöschl, U., Andreae, M. O., Artaxo, P., Jimenez, J. L., Martin, S. T., and Wang, J.: CCN activity and organic hygroscopicity of aerosols downwind of an urban region in central Amazonia: seasonal and diel variations and impact of anthropogenic emissions, Atmos. Chem. Phys., 17, 11779-11801, https://doi.org/10.5194/acp-17-11779-2017, 2017.

Tokay, A., and Short, D. A.: Evidence from tropical raindrop spectra of the origin of rain from stratiform versus convective clouds, J. Appl. Meteor., 35, 355–371, 1996.

Tokay, A., Petersen, W.A., Gatlin, P., and Wingo, M.: Comparison of raindrop size distribution measurements by collocated disdrometers, J. Atmos. Ocean. Technol., 30, 1672–1690, 2013.

Vila, D. A., Machado L. A. T., Laurent H., and Velasco, I.: Forecast and Tracking the Evolution of Cloud Clusters (ForTraCC) using satellite infrared imagery: Methodology and validation, Wea. Forecasting, 23, 233-245, doi: 10.1175/2007WAF2006121.1, 2008.

Wang, D., Giangrande, S. E., Bartholomew, M. J., Hardin, J., Feng, Z., Thalman, R., and Machado, L. A.: The Green Ocean: Precipitation Insights from the GoAmazon2014/5 Experiment, Atmos. Chem. Phys. Discuss., https://doi.org/10.5194/acp-2018-101, in review, 2018.

Wang, J., Krejci, R., Giangrandel, S., Kuang, C., Barbosa, H. M. J., Brito, J., Carbone, S., Chi, X. G., Comstock, J., Ditas, F., Lavric, J., Manninen, H. E., Mei, F., Moran-Zuloaga, D., Pohlker, C., Pohlker, M. L., Saturno, J., Schmid, B., Souza, R. A. F., Springston, S. R., Tomlinson, J. M., Toto, T., Walter, D., Wimmer, D., Smith, J. N., Kulmala, M., Machado, L. A. T., Artaxo, P., Andreae, M. O., Petaja, T., and Martin, S. T.: Amazon boundary layer aerosol concentration sustained by vertical transport during rainfall, Nature, 539, 416–419, 2016.

Weigel, R., Spichtinger, P., Mahnke, C., Klingebiel, M., Afchine, A., Petzold, A., Krämer, M., Costa, A., Molleker, S., Reutter, P., Szakáll, M., Port, M., Grulich, L., Jurkat, T., Minikin, A., and Borrmann, S.: Thermodynamic correction of particle concentrations measured by underwing probes on fast-flying aircraft, Atmos. Meas. Tech., 9, 5135-5162, doi:10.5194/amt-9-5135-2016, 2016.

Wendisch, M., and Brenguier, J. L. (Eds.): Airborne Measurements for Environmental Research: Methods and Instruments. Wiley-VCH Verlag GmbH & Co. KGaA, Weinheim, Germany. ISBN: 978-3-527-40996-9, doi:10.1002/9783527653218, 2013.

Wendisch, M., et al: The ACRIDICON-CHUVA campaign: Studying tropical deep convective clouds and pre-cipitation over Amazonia using the new German research aircraft HALO. Bull. Am. Meteorol. Soc., 97, 10, 1885-1908, http://dx.doi.org/10.1175/BAMS-D-14-00255.1, 2016.

Williams, E., and Coauthors: Contrasting convective regimes over the Amazon: Implications for cloud electrification, J. Geo- phys. Res., 107, doi:10.1029/2001JD000380, 2002

Zhuang, Y., Fu, R., Marengo, J. A., and Wang, H.: Seasonal variation of shallow-to-deep convection transition and its link to the environmental conditions over the Central Amazon, J. Geophys. Res. Atmos., 122, https://doi.org/10.1002/2016JD025993, 2017.

.

Figure captions

Figure 1: ~~.~~ Rainfall rate (RR) histogram for wet and dry seasons computed using the T3 disdrometer. Wet and dry seasons occurred from January to March and August to October, respectively, for the years 2014 and 2015. Rainfall rate (RR) and total rainfall (R) are given in the legend~~Rain rate histogram for wet and dry seasons computed using the disdrometer in T3 site. Wet and dry seasons covered the periods between January to March and August to October, respectively, for the years 2014 and 2015. Rain rate (RR) and total rainfall (R) are given in the legend.~~

Figure 2: Box Plots illustrating monthly a) convective available potential energy (CAPE), b) convective inhibition energy (CINE), c) precipitable water vapour (PWV), d) lifting condensation level (LCL), e) bulk shear and f) mean rainfall rate (RR) and rainfall. Data are for 2014 and were collected at 00, 06, 12 and 18 UTC using the T3 radiosondes. Rainfall was computed using the T3 rain gauge. Each box represents the 25% to 75% populations and the line inside the box shows the median value; circles represent outliers.~~Box Plot of the monthly statistics of the a) convective available potential energy (CAPE), b) convective inhibition energy (CINE), c) precipitable water vapor (PWV), d) lifting condensation level (LCL), e) bulk shear and f) rain rate and rainfall monthly mean. Calculations are for 2014 using the T3 radiosondes at 00, 06, 12 and 18 UTC. Rainfall was computed using the T3 raingauge. The box represents the 25% to 75% populations and the line inside the box shows the median value, and the circles are the outliers.~~

Figure 3: Rain cell (left, based on the SIPAM S-band radar) and cloud cluster (right, based on GOES-13 IR brightness temperature [B_T]) size distributions~~, on the left and right side respectively,~~ between wet and dry seasons; and the difference between dry and wet season distributions (in black, right axis)

Figure 4: Mass-weighted mean raindrop diameter (D_m) as a function of the rainfall rate (RR) for wet and dry seasons for a) convective and b) stratiform rain events. The arrows on the x-axis indicate variations in the averages based on the Student's t-test (95% confidence). The box represents the 25% to 75% populations and the line inside the box shows the median value; the circles are the outliers.~~Raindrop mean mass-weighted diameter (D_m) as a function of the rain rate (from radar S-band) for wet and dry seasons for a) convective and b) stratiform rain events. The arrows on the x-axis indicate that the averages are different, based on the Student's t-statistic at 95% confidence. The box represents the 25% to 75% populations and the line inside the box shows the median value, and the circles are the outliers.~~

Figure 5: X-band radar reflectivity contoured frequency by altitude diagram (CFAD) for the wet (top) and dry (bottom) seasons. Each CFAD consists of a PDF of reflectivity (2 dBZ bin intervals) at each height (400 m bin intervals) multiplied by 100 so that values are displayed as a percentage.~~X-band radar reflectivity contoured frequency by altitude diagram (CFAD) for the dry and wet seasons from the X-band radar.~~

Figure 6:

ZDR (gives an idea o~~f hf~~ horizontal~~-~~positively~~-~~ ~~-~~and vertical~~-~~negatively~~-~~ ~~-~~oriented hydrometeors), KDP (gives an idea of hydrometeor concentration and hydrometeor orientation) and horizontal-vertical correlation (gives an idea of the

homogeneity of the hydrometeor) contoured frequency by altitude diagram (CFAD) for the wet (top) and dry (bottom) seasons as derived using the X-band radar. Each CFAD consists of a PDF of ZDR (0.5 dB bin intervals), KDP (0.5 dB bin intervals) and co-polar correlation (0.05 bin intervals) at each height (400 m bin intervals) multiplied by 100 so that the values are displayed as a percentage.

~~ZDR (gives an idea about horizontal – positive and vertical – negative oriented hydrometeor), KDP (gives an idea about the hydrometeor concentration and hydrometeor orientation) and horizontal-vertical correlation (gives an idea about the hydrometeor homogeneity) contoured frequency by altitude diagram (CFAD) for the dry and wet seasons from the X-band radar. Each CFAD consists of a PDF of Zdr (0.5 dB bin intervals), Kdp (0.5 dB bin intervals) and co-polar correlation (0.05 bin intervals) at each height (400 m bin intervals) multiplied by 100 so that values are in percent.~~

Figure 7: Mass-weighted mean rainfall diameter as a function of the rainfall rate (RR) during the wet season for clean (CPC smaller than the 33rd percentile) and polluted (CPC larger than the 66th percentile) air over pasture. Each box represents the 25% to 75% populations, and the line inside the box shows the median value; circles represent outliers.~~Rainfall mean mass-weighted diameter as a function of the rain rate during the wet season for clean (CPC smaller than the 33rd percentile) and polluted (CPC larger than the 66th percentile) over pasture. The box represents the 25% to 75% populations, and the line inside the box shows the median value, and the circles are the outliers.~~

Figure 8: a) Four vegetation classes, as obtained from the digital Terra-Class classification: forest, hydrography, non-forest, and urban area; and b) Topography across a 150 km radius as derived using SIPAM radar. X-band~~-band~~ (T3 site) and S-band ~~band~~ radar positions are shown in the figure.~~**a)** The vegetation classes obtained from the digital Terra-Class classification in four specific classes: forest, hydrography, non-forest, and urban area and b) Topography over the 150 km radius of the SIPAM radar. X band (T3 site) and S band radar position are shown in the figure.~~

Figure 9: Rainfall rate (RR; from S-band radar) box plots for the wet and dry seasons given different surface cover classes. Each box represents the 25% to 75% populations, and the line inside the box represents the median value.~~Rain rate (from radar S-band) box plot statistics for the wet and dry seasons for different surface cover classes. The box represents the 25% to 75% populations, and the line inside the box shows the median value.~~

Figure 10: AC17 flight paths over forested and deforested regions. Flight legs 1 and 2 are shown in red on panels (A) and (C), respectively (source from Google Earth). The dot on the flight leg 1 corresponds to 56°57'W, 4°13'S and that on flight leg 2 corresponds to 55°17'W, 5°53´S. Visible GOES-13 images for flight legs 1 and 2 at the time of each flight are shown on panels (B) and (C), respectively.~~AC17 flight paths over forested and deforested regions. The flight leg is shown in red (source from Google Earth), the upper(A) panel is leg#1, and the (C) panel is leg#2. The dot in the flight leg corresponds to 56°57'W, 4°13'S for leg#1 and 55°17'W, 5°53´S for leg#2. Visible GOES-13 images at the time of the flights are shown on panel (B) for leg#1 and (C) leg#2 flights.~~

Figure 11: a) Cloud droplet concentration as a function of liquid water content; b) mass-weighted mean cloud diameter as a function of vertical velocity; and c) cloud droplet concentration as a function of vertical velocity for forest and pasture at

different heights.~~a) Cloud droplet concentration as a function of the liquid water content; b) cloud mean mass-weighted diameter as a function of the vertical velocity; and c) cloud droplet concentration as a function of the vertical velocity for forest and pasture at different heights.~~

Figure 12: CCN concentration (N_{CCN}) cumulative histogram for (a) leg 1 and (b) leg 2 of AC17 flight paths over forested and non-forested regions at different flight heights.~~CCN number concentration (N_{CCN}) Cumulative histogram for leg1 (a) and leg2 (b) for AC17 flight paths over forest and non-forest regions for different flight heights.~~

Figure 13: Wet and dry season rainfall rate (RR) box plots for different topography classes. Each box represents the 25% to 75% populations, and the line inside the box represents the median value. The line represents the remaining population.~~Rain rate box plot statistics for the wet and dry seasons for different topography classes. The box represents the 25% to 75% populations, and the line inside the box shows the median value. The line represents the remaining population.~~

Figures

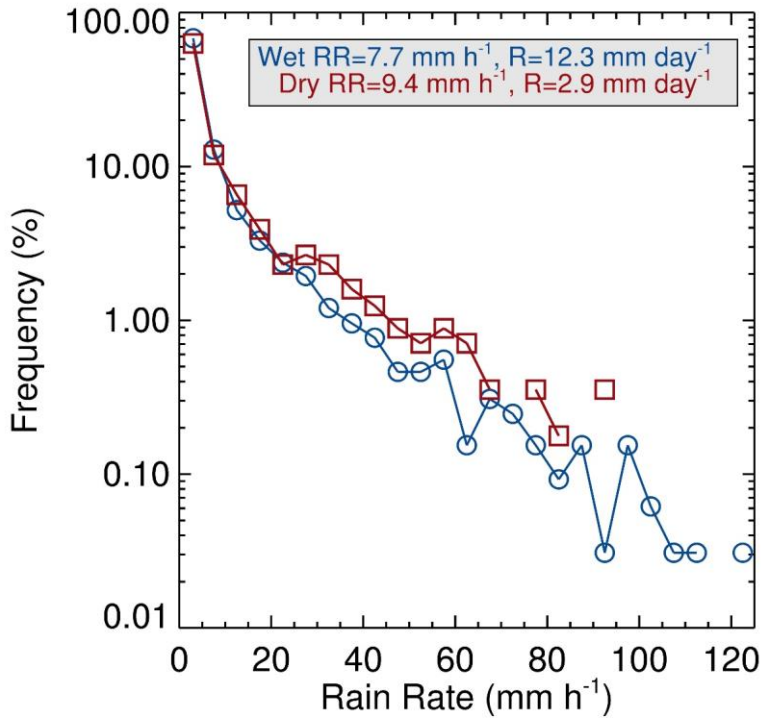

Figure 1. Rainfall rate (RR) histogram for wet and dry seasons computed using the T3 disdrometer ~~in T3 site~~. Wet and dry seasons ~~covered the periods between~~occurred from January to March and August to October, respectively, for the years 2014 and 2015. Rainfall rate (RR) and total rainfall (R) are given in the legend.

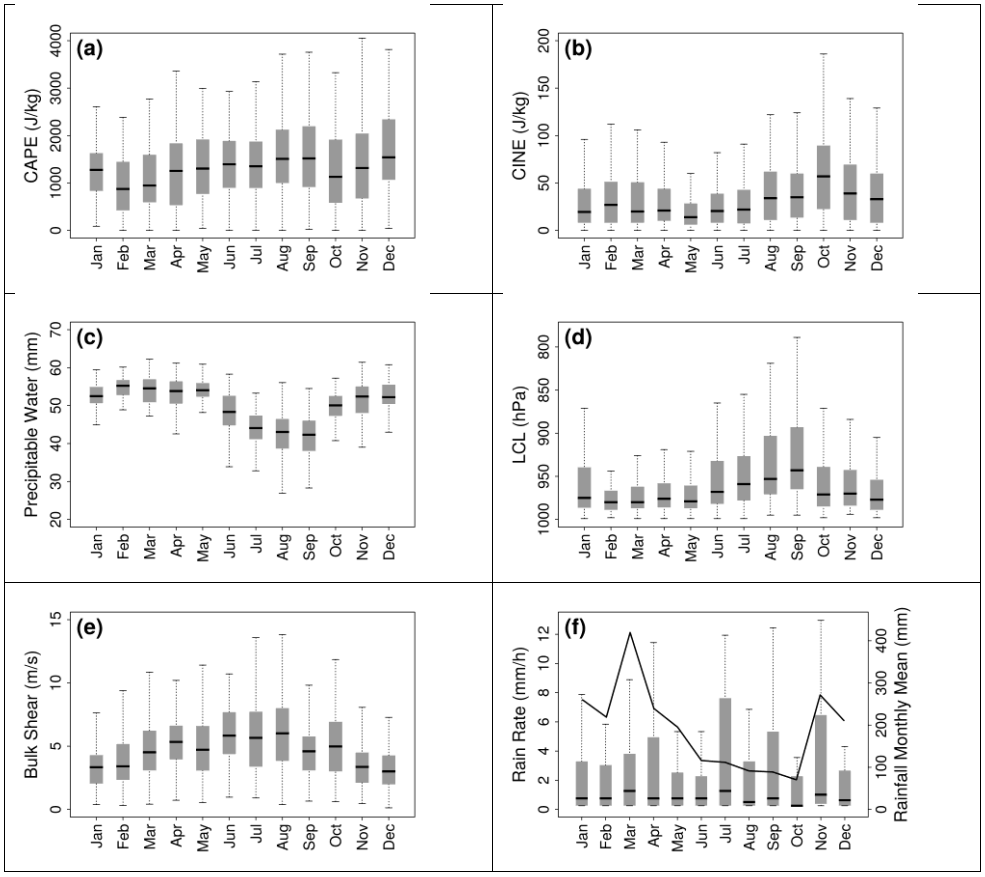

Figure 2: Box Plots illustrating ~~of the~~ monthly ~~statistics of the~~ a) convective available potential energy (CAPE), b) convective inhibition energy (CINE), c) precipitable water vapour (PWV), d) lifting condensation level (LCL), e) bulk shear and f) mean rainfall rate (RR) and rainfall ~~monthly mean~~. Data~~Calculations~~ are for 2014 and were collected ~~using the T3 radiosondes~~ at 00, 06, 12 and 18 UTC using the T3 radiosondes. Rainfall was computed using the T3 rain gauge. Each~~The~~ box represents the 25% to 75% populations and the line inside the box shows the median value; ~~, and the~~ circles represent~~are the~~ outliers.

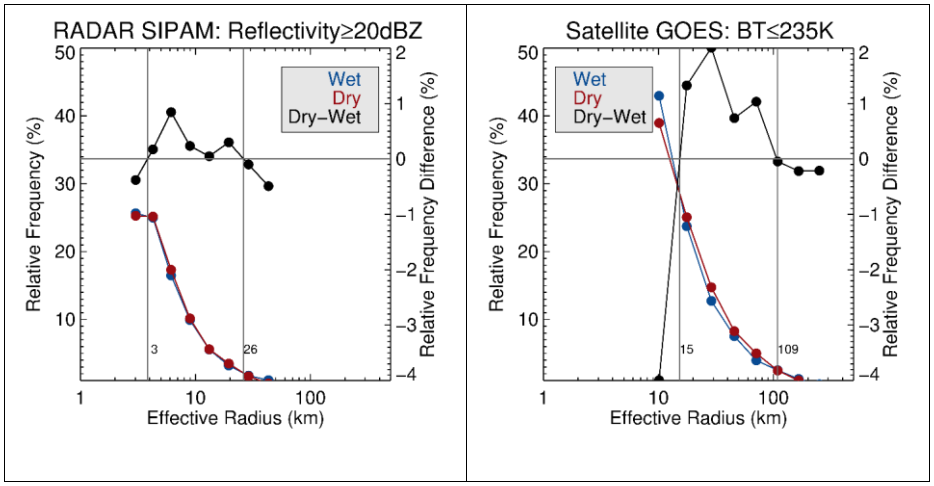

Figure 3: Rain cell (left, based on the SIPAM S-band radar) and cloud cluster (right, based on GOES-13 IR brightness temperature [B_T]) size distributions during the wet and dry seasons; and the difference between the dry and wet season distributions (in black, right axis)

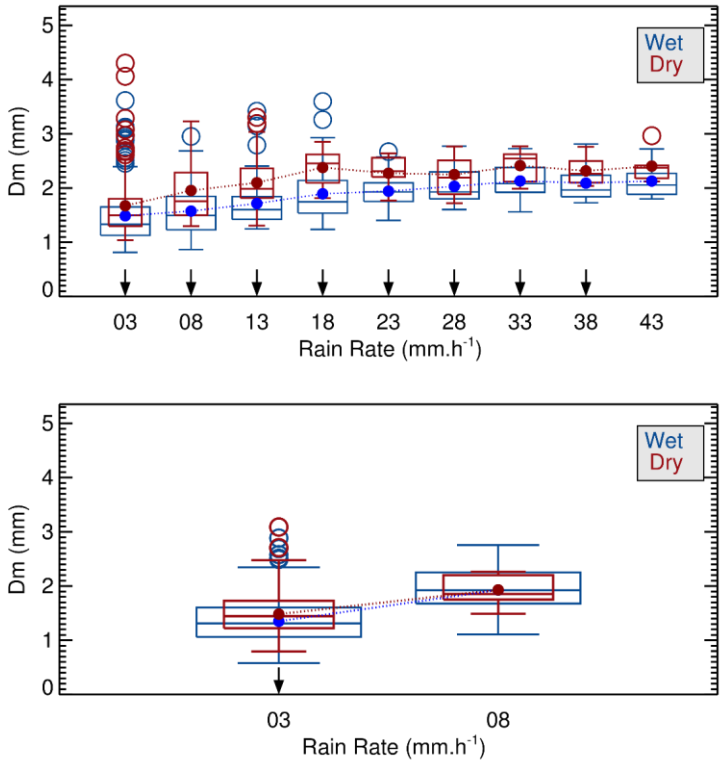

Figure 4: Mass-weighted mean r~~R~~aindrop ~~mean mass-weighted~~ diameter (D_m) as a function of the rainfall rate (RR) for wet and dry seasons for a) convective and b) stratiform rain events. The arrows on the x-axis indicate variations in~~that~~ the averages ~~are different,~~ based on the Student's t-test ~~at~~ (95% confidence). The box represents the 25% to 75% populations and the line inside the box shows the median value~~, and~~ the circles are the outliers.

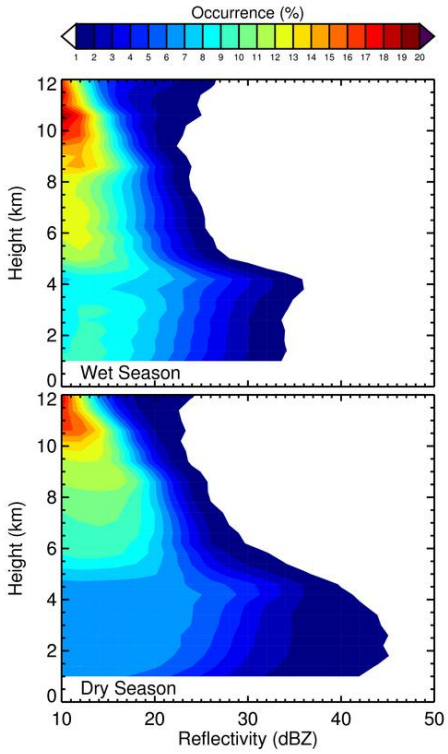

Figure 5: X-band radar reflectivity contoured frequency by altitude diagram (CFAD) for the ~~dry and~~ wet (top) and dry (bottom) seasons ~~from the X-band radar~~. Each CFAD consists of a PDF of reflectivity (2 dBZ bin intervals) at each height (400 m bin intervals) multiplied by 100 so that values are displayed as a percentage~~in percent~~.

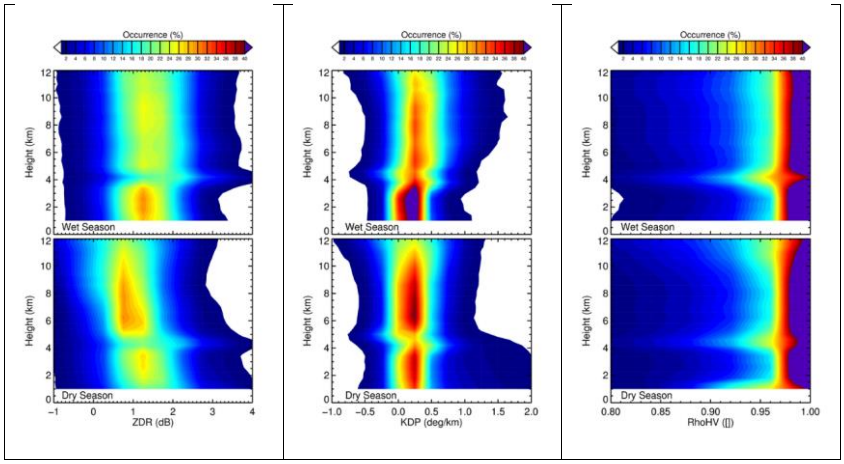

Figure 6: ZDR (gives an idea of ~~about~~ horizontal~~-~~positive~~ly~~ ~~and vertical~~-~~negative~~ly ~~oriented hydrometeor~~s), KDP (gives an idea of~~about the~~ hydrometeor concentration and hydrometeor orientation) and horizontal-vertical correlation (gives an idea of~~about~~ the homogeneity of the hydrometeor ~~homogeneity~~) contoured frequency by altitude diagram (CFAD) for the ~~dry and~~ wet (top) and dry (bottom) seasons as derived using~~from~~ the X-band radar. Each CFAD consists of a PDF of ZDR~~dr~~ (0.5 dB bin intervals), KDP~~dp~~ (0.5 dB bin intervals) and co-polar correlation (0.05 bin intervals) at each height (400 m bin intervals) multiplied by 100 so that the values are displayed as a percentage~~in percent~~.

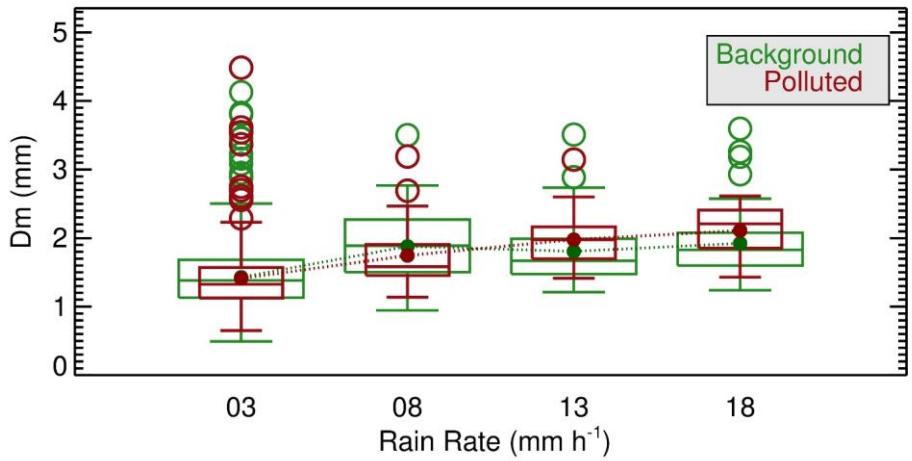

Figure 7: Mass-weighted mean r~~R~~ainfall ~~mean mass-weighted~~ diameter as a function of the rainfall rate (RR) during the wet season for clean (CPC smaller than the 33rd percentile) and polluted (CPC larger than the 66th percentile) air over pasture. Each~~The~~ box represents the 25% to 75% populations, and the line inside the box shows the median value;~~, and the~~ circles ~~are the~~represent outliers.

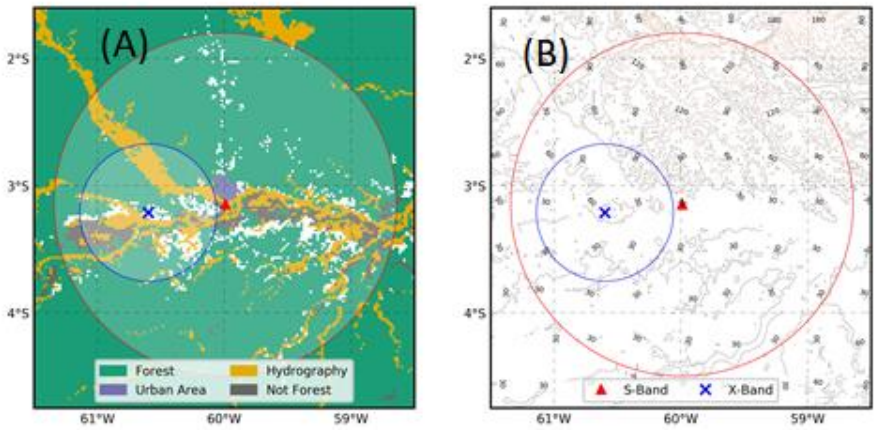

Figure 8: a) Four v~~The v~~egetation classes, as obtained from the digital Terra-Class classification ~~in four specific classes~~: forest, hydrography, non-forest, and urban area; and b) Topography ~~over the~~across a 150 km radius as derived using~~of the~~ SIPAM radar. X-band (T3 site) and S-band radar positions are shown in the figure.

Formatado: Fonte: Não Negrito

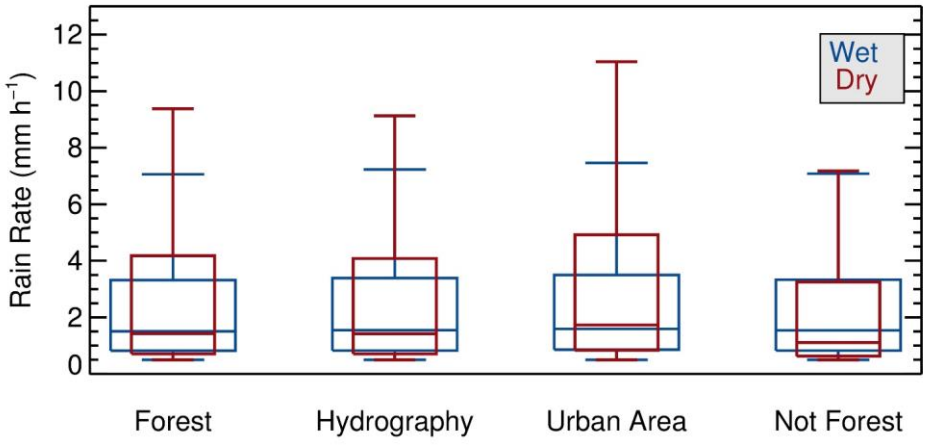

Figure 9: Rainfall rate (from ~~radar~~ S-band radar) box plot~~s statistics~~ for the wet and dry seasons ~~for~~given different surface cover classes. Each~~The~~ box represents the 25% to 75% populations, and the line inside the box ~~shows~~ represents the median value.

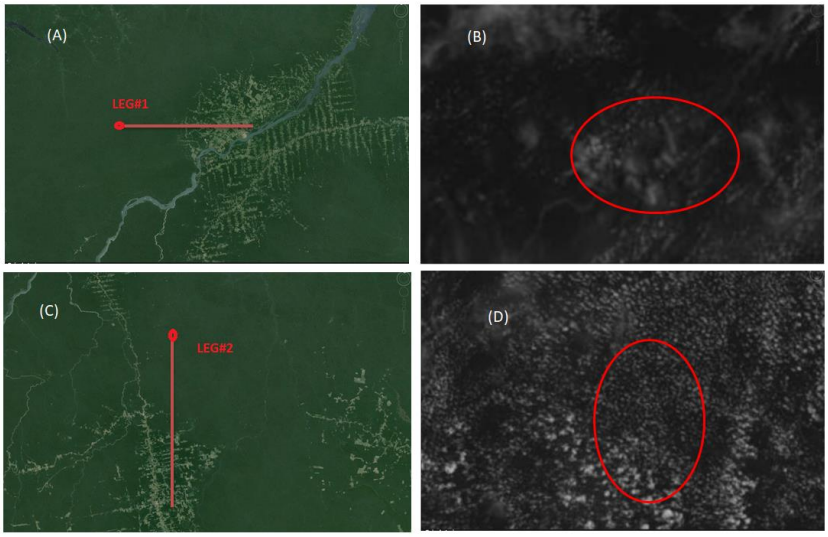

Figure 10: AC17 flight paths over forested and deforested regions. F~~The f~~light legs 1 and 2 are ~~is~~ shown in red on panels (A) and (C), respectively (source from Google Earth)~~, the upper(A) panel is leg#1, and the (C) panel is leg#2~~. The dot on~~in~~ the flight leg 1 corresponds to 56°57'W, 4°13'S ~~for leg#1~~ and that on flight leg 2 corresponds to 55°17'W, 5°53´S ~~for leg#2~~. Visible GOES-13 images for flight legs 1 and 2 at the time of each~~the~~ flight~~s~~ are shown on panels (B) ~~for leg#1~~ and (C), respectively ~~leg#2 flights~~.

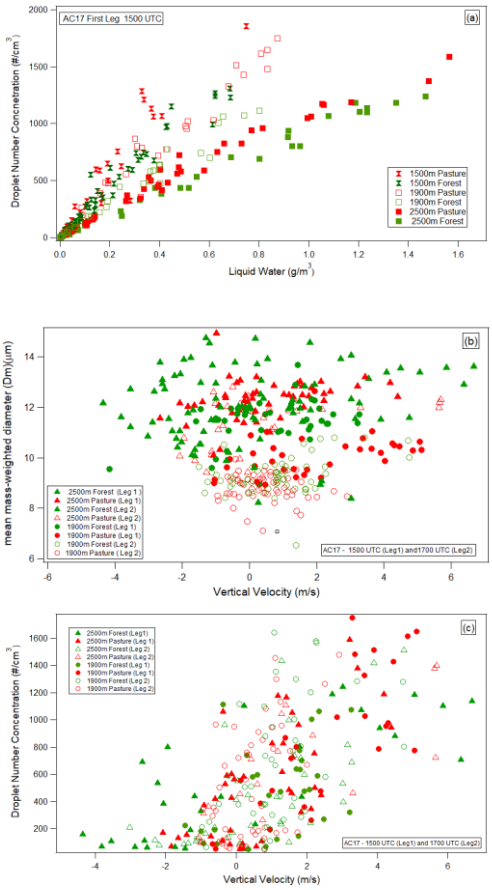

Figure 11: a) Cloud droplet concentration as a function of ~~the~~ liquid water content; b) ~~cloud mean~~ mass-weighted mean cloud diameter as a function of ~~the~~ vertical velocity; and c) cloud droplet concentration as a function of ~~the~~ vertical velocity for forest and pasture at different heights.

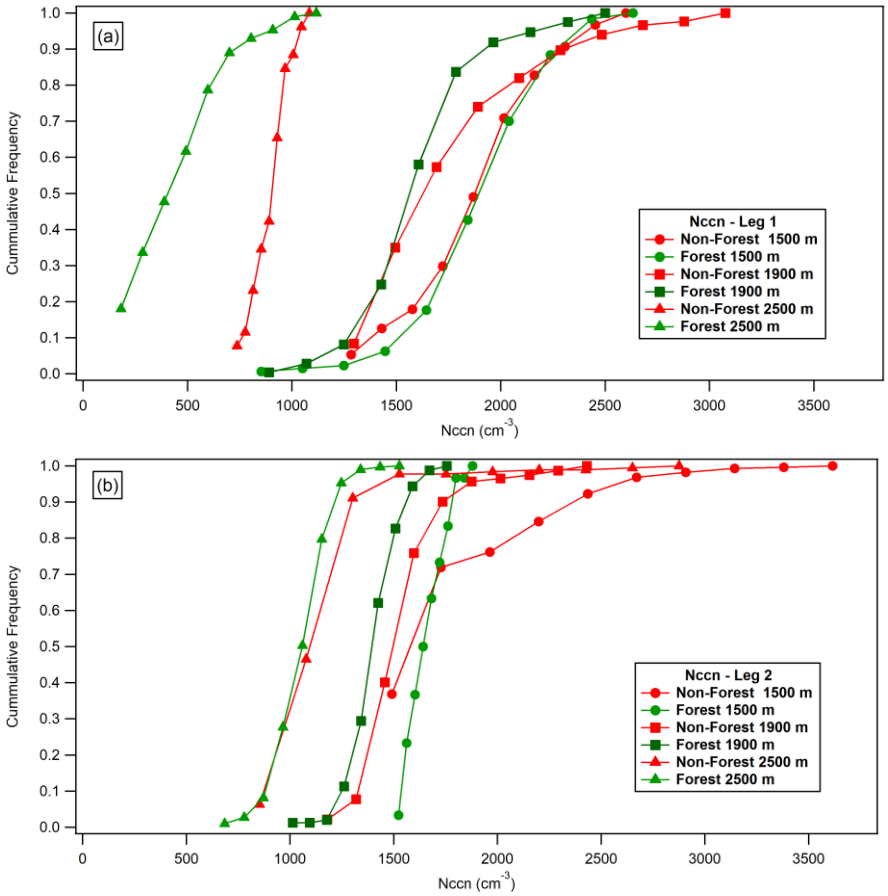

Figure 12: CCN ~~number~~ concentration (N_{CCN}) c~~C~~umulative histogram for (a) leg 1 ~~(a)~~ and (b) leg 2 of~~(b) for~~ AC17 flight paths over forested and non-forested regions at~~for~~ different flight heights.

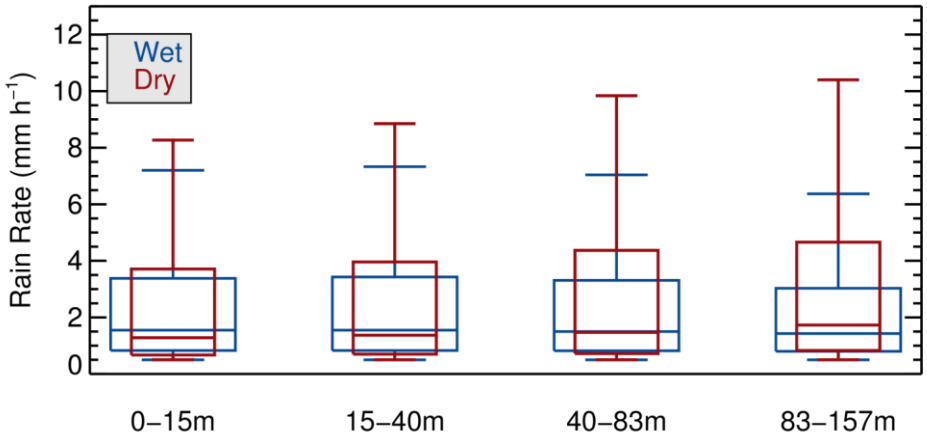

Figure 13: Wet and dry season r~~R~~ainfall rate box plots~~ statistics for the wet and dry seasons~~ for different topography classes. Each~~The~~ box represents the 25% to 75% populations, and the line inside the box ~~shows~~ represents the median value. The line represents the remaining population.